more than 4000 in affected individuals, and is correlated with disease severity and inversely correlated with the age at onset (Harley et al., 1992; Ashizawa et al., 1992). The clinical expression of DM1 includes myotonia and progressive muscle weakness, frontal baldness, cataracts, cardiac conduction defects, hypogonadism, endocrine deficiency and cognitive impairment (Harper 1989). A neurodegenerative process is often observed in the brain of aged DM1 patients (Vermersch et al., 1996; Kiuchi et al., 1991, Oyamada et al., 2006), characterized by the presence of neurofibrillary tangles in the neocortex and in the subcortical nuclei. These neurofibrillary tangles consist of the intraneuronal aggregation of abnormally modified microtubule-associated Tau proteins.

The etiology of DM1 implies that the disease is due to an RNA gain-of-function. CUG repeats accumulate in the nucleus in the form of ribonuclear inclusions, named foci (Taneja et al., 1995). These ribonuclear inclusions contain several proteins, among which the Muscleblind-like 1 (MBNL1) protein is predominant (Mankodi et al. 2001, Jiang et al., 2004). The sequestration of MBNL1 leads to the loss of its function. The disruption of the mouse *MBNL1* gene thus reproduces the trans-dominant effect of the CUG repeats (Kanadia et al. 2003), which in turn results in the modified splicing of a growing list of transcripts, including cardiac troponin T (cTNT), the insulin receptor (IR), the muscle-specific chloride channel (CIC-1), myotubularin-related protein 1, fast skeletal troponin T, the NMDA NR1 receptor, ryanodine receptor 1, the amyloid beta precursor protein and Tau (Jiang et al. 2004, Kanadia et al. 2003, Savkur et al. 2001, Sergeant et al., 2001, Buj-Bello et al., 2002, Charlet et al. 2002, Lin et al. 2006, Kimura et al. 2005).

In *Drosophila*, in which they were initially characterized, Muscleblind proteins have been shown to be required for the terminal differentiation of myocytes and photoreceptors (Begemann et al. 1997, Artero et al., 1998); for review see (Pascual et al., 2006)). In humans, the MBNL genes consist of three paralogous: MBNL1, MBNL2 and MBNL3. MBNL1 and MBNL2 are found in numerous tissues, with MBNL1 expression at its strongest in muscle and the heart (Miller et al. 2000). MBNL3 is mostly expressed in the placenta. The human *MBNL1* gene is located on chromosome 3, and alternative splicing generates several isoforms (Mankodi et al. 2001, Miller et al. 2000; Kino et al., 2004; Fardaei et al. 2002), which have been characterized in skeletal muscle (Kanadia et al. 2006).

MBNL1 proteins regulate the splicing of both cTNT and IR pre-mRNAs (Ho et al., 2004). Some MBNL1 isoforms also bind double-stranded RNA, a property that might be in balance with their role as a modulator of transcript splicing. The presence of the sequence encoded by exon 4 is essential for MBNL1 to bind to CUG repeats (Kino et al., 2004). Together, these results suggest a dual, and possibly interrelated, function for MBNL1 isoforms, as double-stranded RNA binding proteins, and as trans-regulatory splicing factors.

Although MBNL1 has been characterized in skeletal muscle to some extent (Kanadia et al., 2006), little is known about its expression in the brain, under either normal or pathological conditions. The aim of the present work was to study the expression of MBNL1 in the brain of DM1 patients and control individuals, as well as its relationship to Tau splicing. We show here that a fetal isoform of MBNL1 is overexpressed in the brain tissue of DM1 patients. The expression of this fetal isoform can be reproduced by the ectopic expression of long CUG repeats *in vitro*. We also show that the Tau mis-splicing observed in DM1 is reproduced by the ectopic expression of CUG repeats or the RNA interference-mediated inactivation of MBNL1. In contrast, the expression of adult or fetal MBNL1 isoforms does not affect Tau exon 2/3 inclusion. Taken together, our results suggest that in the DM1 brain, MBNL1 and Tau splicing are targets of the trans-dominant effect of CUG repeats and that the silencing of MBNL1 results in alterations in Tau splicing.

Materials and methods

Human brain tissue samples

DM1 brain tissue samples were obtained at autopsy from 3 patients aged of 42, 53 and 64 years. Two patients (DM1.1 and DM1.3) had an adult form of DM1, while the third had a congenital form of DM1 (DM1.2). These cases have been previously described (Leroy et al., 2006a). Three control individuals were included in the study. The brain tissues were obtained from the Department of Neurology, University Hospital Centre of Lille, France, in accordance with the protocol of the local ethics committee. Post-mortem delays were below 48 h, and brain tissue was stored at −80 °C. Four cortical brain regions, the temporal, occipital, frontal and parietal, were dissected for analysis. The genetic diagnosis of DM1 was confirmed by a long PCR assay. For the analysis of the expression of different human MBNL1 transcripts during an early stage of development, we analyzed first strand cDNA preparations from a human fetal brain (Human fetal MTC™ panel, BD Biosciences, Clontech, California, USA).

Semi-quantitative analysis

Total RNA was isolated from brain tissue using RNAgents (Promega, France) according to the manufacturer's instructions. Total RNA was isolated from cells using the Nucleospin® RNA II kit (Macherey Nagel, Düren, Germany). RNA concentration was determined by absorption at 260 nm. RT-PCR was performed in triplicate with 1 μg of total RNA using random hexamers (5 μM/l) and the M-MLV reverse transcriptase (Promega, France) according to standard protocols. No DNA amplification was observed in the RT controls. PCR was carried out in a final volume of 25 μl, with 15 pM of each primer (primer sequences are detailed in Table 1), 1.5 mM $MgCl_2$ and 1 U of Taq polymerase (Invitrogen), under the following conditions: 5 min at 94 °C, 22 to 30 cycles of a 1 min denaturation step at 94 °C, annealing for 2 min at the temperature indicated in Table 1, 2 min of extension and 7 min of final extension at 72 °C. GAPDH was used as an internal control. The reaction products were resolved by electrophoresis using a 4% or 5% polyacrylamide gel, and bands were stained with SYBR Gold (Molecular Probes, Oregon, USA). The intensity of SYBR Gold luminescence was measured using a FluorolmagerTM scanner (Claravision, France). The mRNA signals were normalized to that of GAPDH mRNA.

Table 1
Primers and PCR reactions

Sequence amplified	Sense primers	(Exon location)	Antisense primers	(Exon location)	PCR conditions	Fragment size (bp)
$MBNL1_{41/43}$	5′-ATTACAACCCGTGCCAATGT-3′	(3/4)	5′-CACCATGGGAACAACACTTGTA-3′	(8/9)	1.0 mM $MgCl_2$ 60 °C	676/730
$MBNL1_{40/42}$	5′-CCCCATTACAACCCGTGCCAAT-3′	(3/4)	5′-ATGGGAACTGGTGGGAGAA-3′	(7/9)	1.5 mM $MgCl_2$ 60 °C	640/694
MBNL1 exon 5	5′-AATTGCAACCGAGGAGAAAA-3′	(5)	5′-CAGCCTGGTTGACCTGGTAT-3′	(5)	1.5 mM $MgCl_2$ 60 °C	199
MBNL1 exon 6	5′-AATTGCAACCGAGGAGAAAA-3′	(5)	5′-AGGGGTCGCTTCAGTGATTT-3′	(6)	1.5 mM $MgCl_2$ 60 °C	269
MBNL1 exon 8	5′-CAAAGAGGCCTGCTCTTGAA-3′	(7)	5′-CAACACTTGGTAGCGGGTGC-3′	(8)	1.5 mM $MgCl_2$ 60 °C	159
MBNL1 exon 6–8	5′-GCAACCTTTGACCTGGGAAT-3′	(6/7)	5′-ATTGAGCCTGGTGGGAGAA-3′	(7/8)	1.5 mM $MgCl_2$ 60 °C	167
MBNL1 exon 3–11	5′-ACTAGCCAATGCCATGATGC-3′	(3)	5′-TTGTGGCTAGTCAGATGTTCG-3′	(11)	1.5 mM $MgCl_2$ 60 °C	588–882
hcTNT exon 5	5′-CATTCACCACATTGGTGTGC-3′		5′-AGGTGCTGCCGCCGGGCGGTGGCTG-3′		1.5 mM $MgCl_2$ 64 °C	109, 139
Tau exon 2/3	5′-TACGGGTTGGGGGACAGGAAAGAT-3′	(1)	5′-GGGGTGTCTCCAATGCCTGCTTCT-3′	(4)	1.5 mM $MgCl_2$ 65 °C	112, 199, 286
DMPK 3′UTR	5′-TGTCTGTCCCCACCTAGGAC-3′		5′-GCTAGCTCCTCCCAGACCTT-3′		1.5 mM $MgCl_2$ 60 °C	171
GAPDH	5′-CCATGGCACCGTCAAGGCTGA-3′		5′-GCCAGTAGAGGCAGGGATGAT-3′		1.5 mM $MgCl_2$ 62 °C	440

List of primers used to analyze the expression of MBNL1 isoforms and the alternative splicing of Tau exon 2 and 3 and hcTNT exon 5. The first column indicates the sequences that were amplified. The second and third columns are the sequence of the forward and reverse primers used, and their exonic location. The concentration of $MgCl_2$, annealing temperature and size of the fragments are also indicated.

Real time RT-PCR

The expression levels of MBNL1 exon 6, exon 8 and exon 5 were studied by real time RT-PCR. The primers used are indicated in Table 1. We analyzed the expression of MBNL1 transcripts containing both exon 6 and exon 8 (exons 6–8) using a forward primer overlapping exons 6 and 7, and a reverse primer overlapping exons 7 and 8 (Table 1). The levels of MBNL1 were assessed relative to the level of β-actin. The PCR was performed with a Light Cycler (Roche, Mannheim, Germany). The master mix contained Taq DNA polymerase and SYBR Green I dNTPs (Light Cycler® FastStart DNA Master SYBR Green, Roche, Mannheim, Germany). The primers were used at a final concentration of 0.5 μM. The conditions required for amplification included 2.5 μM of $MgCl_2$ and annealing at 62 °C for exon 6, and 4 μM of $MgCl_2$ and annealing at 64 °C for exon 8. The amplification of exon 5 and exons 6–8 required 2.5 μM of $MgCl_2$ and annealing at 60 °C, over 40 cycles.

Antiserum production and purification

Antibodies were raised by immunizing rabbits (Eurogentec, Liege, Belgium) with a specific MBNL1 N-terminal peptide, 9-RDTKWLTLEV-18 (numbering according to $MBNL1_{42}$; Swiss-Prot ref. MBNL1_Human Q9NR56), which was coupled at its C-terminal end to keyhole limpet hemocyanin. The specificity of the antiserum was tested using HeLa cells transfected with MBNL1 or non-transfected controls (Kino et al. 2004).

Cloning of MBNL1 isoforms and molecular constructs

To screen for the different MBNL1 isoforms, we selected primers delimiting the coding sequence between exon 2 and exon 11 of MBNL1. These exons are common to the isoforms previously described (Kino et al., 2004). Total cDNA sequences were obtained by amplification of DM1 and control cDNA, with DYNAzyme EXT™ Taq polymerase (Finnzymes, Espoo, Finland). PCR products were cloned into the PCR-TOPO TA Cloning vector (Invitrogen, California, USA) for sequencing. Plasmid DNA was purified using the Nucleobond® AX kit (Macherey Nagel, Düren, Germany). Other plasmids were constructed for each MBNL1 isoform, with the addition of N-terminal GFP and V5-tags to the coding sequence. Briefly, MBNL1 cDNAs in TOPO vectors were subcloned into the Gateway® system (Invitrogen) and inserted into pDEST 53-GFP and pcDNA 3.1-nV5. All constructs were double-strand sequenced. Plasmids containing the 3′UTR of DMPK with 5 or 200 CTG repeats were derived from previously described constructs under a rodent ROSA promoter (Amack et al., 1999). The constructs were subcloned into pcDNA 3.1 under the control of the CMV promoter; the empty pcDNA plasmid was used as a control during transfection. The plasmid containing the 3′UTR of DMPK with 960 interrupted CTGs was a minigene construct also under the control of the CMV promoter. It contained the last 5 exons of DMPK followed by the full length DMPK 3′UTR, with 960 CTG repeats interrupted at every 20th repeat by CTCGA motif (Ho et al., 2005). The conservation of the number of CUG repeats was verified by a long PCR assay. The RTB300 minigene containing

exon 5 of human cTNT (hcTNT) has been previously described (Cooper, 1998).

Cell culture and transfection

HeLa or COS cells were grown in monolayer cultures in 6 well plates in Dulbecco's Modified Essential Medium (DMEM) (Invitrogen, California, USA) supplemented with 10% FBS and 0.5% Penicillin/Streptomycin, at 37 °C in a humidified CO_2 (5%) incubator. Cells grown to ~50% confluence were transiently transfected with 2 μg of plasmid DNA, using the Superfect ExGene 500 transfection reagent (Fermentas), or growing doses of plasmids (from 0.5 to 4 μg). Total RNA was analyzed 48 h post-transfection, with GAPDH as an internal loading standard except where otherwise mentioned. For silencing experiments, siRNAs were synthesized by Eurogentec. The sense strand sequences of the siRNAs designed to target MBNL1 mRNA transcripts were as follows: siMBNL1a 5′-CGCAGUUGGAGAUAAAUGG-3′,

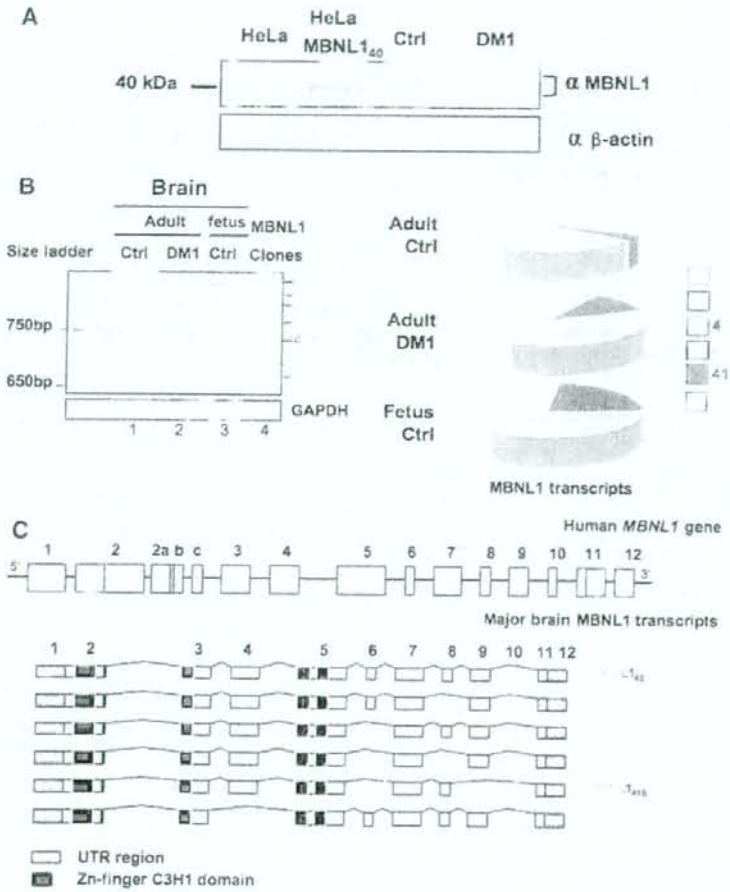

Fig. 1. MBNL1 expression in control and DM1 brain tissues. A. MBNL1 protein expression. Western blotting of protein extracts from untransfected HeLa cells (lane 1) or cells transfected with the MBNL1$_{40}$ expression vector (lane 2). MBNL1 protein expression was also analyzed in control (lane 3) and DM1.3 (lane 4) frontal cortical homogenates. Proteins were transferred onto a nitrocellulose membrane and probed with our MBNL1 antiserum (α MBNL1), then stripped and re-probed with a β-actin antibody (α β-actin). B. MBNL1 transcript expression. Left panel: RT-PCR analysis of total RNA from adult control (lane 1), DM1.3 (lane 2) and fetal control (lane 3) brain tissue using oligonucleotides complementary to MBNL1 exons 3 and 11. Five brain transcripts (36L, 40, 41, 42 and 43) were identified by RT-PCR followed by cDNA cloning and sequencing (lane 4), as described in the Materials and methods. MBNL1$_{41S}$ was identified by isolating the band from the acrylamide gel and sequencing. GAPDH was used as an internal loading standard. Pie chart showing the distribution of the six major MBNL1 transcripts (36L, 40, 41, 41 S, 42 and 43) in the control (Ctrl), DM1 and fetal brain. C. Representation of the *MBNL1* gene and major brain transcripts. The human *MBNL1* gene is located on chromosome 3q25. The MBNL1 primary transcript contains 15 exons. Grey boxes represent untranslated regions (UTRs). Exons are represented as boxes and introns as lines. Exon 1 and part of exon 2 correspond to the 5′UTR. Two thirds of exon 11 and the entire exon 12 encode the 3′UTR. Black boxes represent the four C3H1 type Zinc-finger motifs which bind to RNA. The Zinc-finger motifs are encoded by exons 2, 3 and 5. Only the five major brain transcripts with a molecular mass ranging from 36 to 43 kDa are represented. The nomenclature used corresponds to that of Kino et al. (2004) and Kanadia et al (2006).

and siMBNL1b 5′-CAGACAGACUUGAGGUAUG-3′ (Ho et al., 2004). A scrambled siRNA and an siRNA against β-actin were also designed as controls. The siRNAs were transfected using JetSI®-Endo (Eurogentec) according to the manufacturer's instructions. Growing concentrations were used (1–200 nM) for the dose response effect.

Protein extraction and western blot analysis

DM1 and control brains were homogenized with a Dounce homogenizer in RIPA buffer (50 mM Tris–HCl pH 7.4, 150 mM NaCl, 1 mM EDTA, 1% NP40, 0.5% deoxycholate) with the addition of 1 mM Na_3VO_4, 125 nM okadaic acid, protease and DNAse inhibitors. The resulting homogenates were sonicated, and spun at 13,000 g for 20 min at 4 °C. The supernatants were transferred and the concentration of proteins measured. The pellets were sonicated again, warmed and centrifuged. The supernatants were diluted with Laemmli Buffer with or without RNAse (40 μg/ml ribonuclease A, Fermentas, Canada). The protein extracts (50 μg each) were used for SDS-PAGE (4–12%; Nupage® Bis–Tris gels, Invitrogen, California, USA) and transferred onto Hybond nitrocellulose membranes (G&E Amersham) using the XCell™ II Blot Module (Invitrogen). The proteins were reversibly stained with Ponceau red in order to control for the amount of protein loaded. After blocking with 5% of skimmed milk in TBS-T (20 mM Tris–HCl pH 8.0, 150 mM NaCl and 0.1% Tween-20), the membranes were incubated overnight at 4 °C with MBNL1 antiserum (1:1000) in the same buffer. Membranes were subsequently incubated with a peroxidase-conjugated goat anti-rabbit IgG (Sigma-Aldrich) (1:4000 in the same buffer) and antibody complexes were revealed using ECL™ and Hyperfilms (G& Amersham) according to the manufacturer's instructions.

Immunofluorescence microscopy

HeLa or COS cells were grown in cell culture chamber slides (Labtek) in DMEM supplemented with 10% FBS. HeLa cells were transfected with either $(CTG)_5$-pcDNA or $(CTG)_{960}$-pcDNA alone, or co-transfected with the MBNL1 isoforms pDEST 53GFP-36L, pDEST 53GFP-40, pDEST 53GFP-42 or pDEST 53GFP-43. COS cells were transfected with MBNL1 isoforms alone. After 48 h, cells were fixed with 4% paraformaldehyde in 0.1 M phosphate buffer (PBS) for 30 min at room temperature, and permeabilized with 0.25% Triton X-100 in PBS. After blocking with 1% bovine serum albumin (BSA) in PBS, the fixed cells were incubated for 2 h at room temperature with the primary antibody in PBS with 1% BSA and 0.25% Triton X-100. The anti-GFP antibody was used to probe for the MBNL1 isoforms and to study their localization. After washing, cells were incubated with Alexa Fluor® 568-conjugated secondary antibodies (Invitrogen). Nucleic acids were stained using TOPRO®-3. The coverslips were mounted onto slides with Vectashield (Vector laboratories). Images were acquired with a Leica TCS NT laser scanning confocal microscope. All data were analyzed using Leica image analysis software.

Statistical analyses

Statistical analyses were performed using the non-parametric Mann–Whitney test, with the help of Prism Software (GraphPad Software Inc., San Diego, USA).

Results

MBNL1 protein expression is not decreased in the DM1 brain

To investigate any change in MBNL1 expression in DM1, we first compared the expression of MBNL1 protein in the frontal cortex of control and DM1 brains by western blot analysis using a

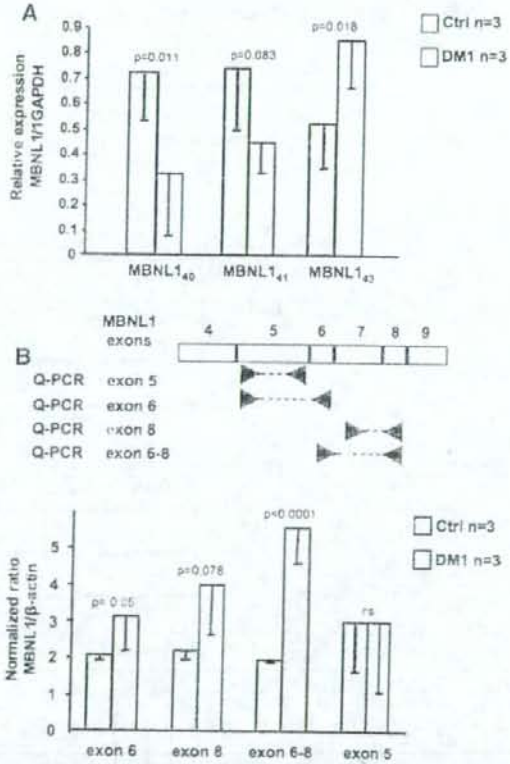

Fig. 2. Semi-quantitative analysis of exon 6 and 8 in control and DM1 tissues. A. Quantification of MBNL1 splice variants by RT-PCR of total RNA from normal and DM1 brain tissues. Primer sets MBNL1$_{41\&43}$ and $_{40\&42}$ (Table 1) were used to amplify selected sets of MBNL1 isoforms. Each primer set simultaneously amplified two transcripts that could be distinguished by their size, according to the insertion or deletion of exon 6. After polyacrylamide gel electrophoresis, the bands were quantified and the results expressed relative to GAPDH, used as an internal loading standard. The histogram represents the mean ± standard deviation of measurements obtained from three different brain samples for each patient. B. Quantitative RT-PCR of MBNL1 transcripts. The relative positions of the primers used are indicated above the histogram in the form of arrows. The first primer set, located in the constitutive exon 5, was used to quantify the total level of MBNL1 transcripts. The other primer sets allowed the specific quantification of MBNL1 transcripts containing exon 6, exon 8 or both exons 6 and 8. Actin was used as the internal standard. All results were obtained from at least three independent experiments.

rabbit polyclonal antibody against the N-terminal region of MBNL1 (see Materials and methods; Fig. 1A). As a control for antibody specificity, we used protein extracts from HeLa cells transfected with the $MBNL1_{40}$ expression vector. A single band at 40 kDa was detected by immunoblotting using our MBNL1 antiserum in these extracts, whereas no immunoreactivity was observed in extracts from non-transfected cells. In extracts from human brain tissue, the antibody revealed a broad band with an apparent molecular mass of 41–43 kDa. No difference in expression levels was seen between control and DM1 brains (Fig. 1A). There did appear to be a slight variation in electrophoretic mobility. However, SDS-PAGE followed by western blotting was insufficient to discriminate between the different MBNL1 isoforms.

MBNL1 splicing is modified and the expression of a fetal isoform increased in the DM1 brain

We analyzed MBNL1 transcript expression in control, DM1 and fetal brain tissues (Fig. 1B), by polyacrylamide gel electrophoresis of the RT-PCR products. As shown in Fig. 1B (lanes 1 and 2) several RT-PCR products were obtained using MBNL1 primers located in exon 3 and 11 (Table 1). After cloning and sequencing, we identified several human MBNL1 isoforms (Fig. 1B, lane 4). The relative distribution of these different MBNL1 brain isoforms is represented in the form of pie charts (Fig. 1C). The major transcripts expressed in the adult control brain are $MBNL1_{40}$, $MBNL1_{41}$ and $MBNL1_{43}$ (Fig. 1B lane 1 and Fig. 1C). In the DM1 brain, $MBNL1_{40}$ and $MBNL1_{41}$ isoforms are significantly less abundant whereas $MBNL1_{43}$ is overexpressed (Fig. 1B, lanes 1–2, and Fig. 1C). Interestingly, we observed that $MBNL1_{43}$ is also one of the major fetal brain transcripts (Fig. 1B, lane 3, and Fig. 1C). The $MBNL1_{43}$ transcript corresponded to the $MBNL1_{42}$ of Kino's classification (Kino et al., 2004), with the addition of exon 8 (Fig. 2D). Such a transcript has also been identified recently by Kanadia et al. in mouse skeletal muscle (Kanadia et al., 2006). $MBNL1_{36L}$ corresponds to $MBNL_{36}$, with the inclusion of the exon 6 sequence (Fig. 2C).

Increased inclusion of MBNL1 exon 6 and 8 in DM1 brain

After qualitative analysis of the pattern of MBNL1 transcript expression in control and DM1 brains, we conducted a semi-

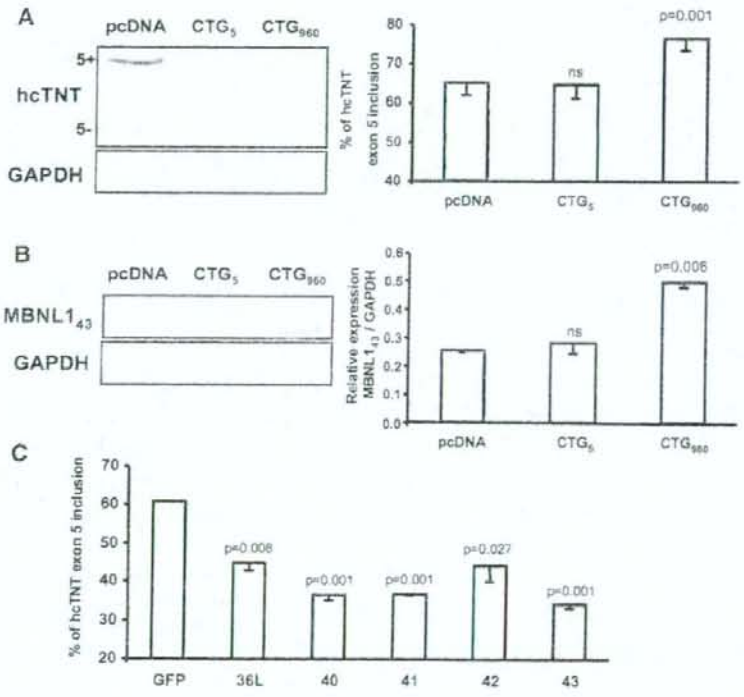

Fig. 3. Effect of long CUG repeats on MBNL1 and hcTNT splicing in HeLa cells. A. Regulation of human hcTNT exon 5 splicing by DMPK 3'UTR CUG repeats. Total RNA was analyzed from HeLa cells co-transfected with the hcTNT minigene and the 3'UTR of human DMPK containing the number of CTG indicated above each lane. The histogram is representative of three individual experiments, and represents the percentage of transcripts that include exon 5. B. Regulation of human MBNL1 by DMPK 3'UTR CUG repeats. Total RNA was analyzed from HeLa cells co-transfected with MBNL1 and the 3'UTR of the human DMPK containing the number of CTG indicated above each line. Results are expressed as the level of $MBNL_{43}$ expression relative to GAPDH. Histograms represent the mean and SD of three individual experiments. C. hcTNT exon 5 inclusion is similarly repressed by several MBNL1 isoforms. HeLa cells were co-transfected with hcTNT minigene and MBNL1 isoforms 36L, 40, 41, 42 or 43, and exon 5 splicing analyzed by RT-PCR. The histogram is representative of three individual experiments and the percentage of transcripts that include exon 5 is expressed as the mean±standard deviation of the three experiments.

quantitative analysis, using three pairs of primers designed to selectively amplify $MBNL1_{40}$, $MBNL1_{41}$ and $MBNL1_{43}$ isoforms (Table 1). The significant increase in $MBNL1_{43}$ ($p=0.018$), and decrease in $MBNL1_{40}$ ($p=0.011$) expression levels (Fig. 2A) confirmed our previous observations (Fig. 1B, pie charts). A decrease in the expression of $MBNL1_{41}$ was also observed, but was not found to be statistically significant (Fig. 2A, $p=0.083$).

$MBNL1_{43}$ contains both exon 6 and exon 8 whereas $MBNL1_{40}$ lacks these exons, suggesting a possible change in the splicing of exon 6 and 8. These exons were quantified as described above, and compared to exon 5, which is constitutive (Fig. 2B). We observed a significant increase in the inclusion of exon 6 ($p=0.05$) between control and DM1 brains. A 2-fold increase in the inclusion of exon 8 was also observed in the DM brain when compared to healthy controls. While this difference was not found to be statistically significant in the current study, subsequent comparisons with a larger number of brains might prove that exon 8 as well as exon 6 are affected in DM1. At the present time, however, the results suggest that the disrupted splicing of MBNL1 is the result of the increased inclusion of exon 6, or of a combination of exon 6 and 8 ($p<0.0001$). It is worth noting that no difference was observed between control and DM1 brains in the level of MBNL1 exon 5 (Fig. 2B), thus confirming previous data showing that the overall expression of MBNL1 was not altered.

Expanded CUG repeats modify MBNL1 splicing and promote the expression of a fetal transcript

The trans-dominant effect of expanded CUG repeats in DM1 has been directly related to the disrupted splicing of several transcripts, such as hcTNT or IR. Based upon the evidence we found for altered MBNL1 isoform expression in the DM1 brain, we asked whether or not the CUG repeats were also responsible for the modified splicing of MBNL1. HeLa cells were used throughout this study. Unlike the neuroblastoma cell lines tested so far (e.g. SY-5Y, N2a, hNT), we observed an alternative splicing of Tau exon 2/3 in HeLa cells. As a positive control for the trans-dominant effect of expanded CUG repeats, the hcTNT minigene was co-transfected with the 3′UTR of human DMPK, containing 5 or 960 CTG repeats expressed under the control of the CMV immediate early promoter (Fig. 3A). The expression of CUG repeats was assessed by RT-PCR of the 3′UTR of DMPK. We also verified that the number of CTG repeats remained unchanged 48 h after transfection (data no shown). A 15% increase in the inclusion of hcTNT exon 5 was observed with CTG_{960}, but not with the CTG_5 minigene. HeLa cells were then transfected with CTG_{960} alone (Fig. 3B) and $MBNL1_{43}$ transcript expression was examined by RT-PCR with the primers $MBNL1_{41/43}$ (Table). In the latter cells, we observed a 1.5 fold increase in the expression of $MBNL1_{43}$ (Fig. 3B), demonstrating that endogenous $MBNL1_{43}$

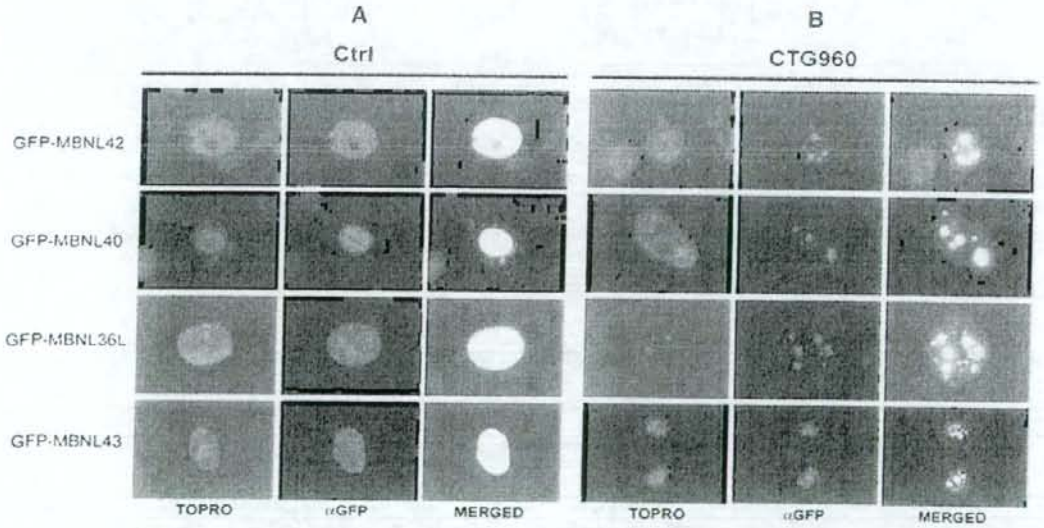

Fig. 4. Intranuclear localization of MBNL1 isoforms in the presence or absence of long CUG repeats. HeLa cells were transfected with GFP–$MBNL_{42}$, GFP–$MBNL_{40}$, GFP–$MBNL_{36L}$ and GFP–$MBNL_{43}$ alone (panel A) or together with pcDNA-CTG_{960} (panel B). In each panel, the first column shows the cell nucleus stained with TOPRO. The second column shows the distribution of the GFP-tagged protein, revealed by an anti-GFP antibody. The last column corresponds to the merged images obtained from TOPRO and anti-GFP staining, showing the localization of MBNL1 isoforms in nuclear RNA foci when co-expressed with long CUG repeats. GFP fluorescence completely overlapped with that observed with an anti-GFP antibody. Cells with a moderate level of expression were selected to illustrate the localization of MBNL1 isoforms, as high cellular expression levels resulted in partial cytosolic localization (data not shown), possibly due to the titration of nuclear import factors.

is overexpressed as a result of the trans-dominant effect of long CUG repeats.

Trans-repression of hcTNT exon 5 inclusion by MBNL1 isoforms, and cellular localization

The modified pattern of MBNL1 isoform expression in DM1 led us to consider whether the MBNL1 isoforms had similar or opposing splicing functions. We examined the trans-regulatory function of these isoforms on hcTNT exon 5 splicing. HeLa cells were co-transfected with the hcTNT minigene and GFP–MBNL1 isoforms (Fig. 3C) or V5–MBNL1 isoforms (data not shown). As a positive control for these constructs, we confirmed the decreased inclusion of hcTNT exon 5 induced by $MBNL1_{40}$ (Fig. 3C). We observed that $MBNL1_{43}$ and $MBNL1_{36L}$ decreased exon 5 inclusion, in a manner similar to $MBNL1_{40}$, $MBNL1_{41}$ and $MBNL1_{42}$.

We next investigated the possibility that another function, such as cell localization or the propensity of CUG repeats to recruit MBNL1 isoforms in nuclear foci, was also modified. All GFP MBNL1 isoforms showed diffuse nuclear staining and were excluded from the nucleoli (Fig. 4A, control panel). We also tested our constructs in COS cells since Lin et al. recently showed that MBNL1 isoform lacking the sequence encoded by exon 7 had a nucleocytoplasmic localization (Lin et al. 2006). $MBNL1_{40}$ isoform which lacks the sequence encoded by exon 7 is localized in the cytoplasm and nucleus of COS whereas the other $MBNL1_{43, 42}$ and $_{36L}$ isoforms, having the exon 7 encoded sequence, were preferentially observed in the nucleus (supplementary Fig. 1). Control HeLa cells transfected with GFP alone or co-transfected with pcDNA-CTG_5 also revealed the diffuse cellular distribution of GFP (data not shown). In contrast, in HeLa cells co-transfected with GFP–MBNL1 isoforms in addition to pcDNA-CTG_{960}, GFP–MBNL1 staining was concentrated at large foci in the nucleus (Fig. 4B), even though the level of protein expression of the GFP–MBNL1 isoforms was found to be invariant between the different experimental groups (western blotting; data not shown).

Loss of MBNL1 expression is responsible for the Tau splicing pattern observed in DM1

We have previously described the preferential expression and aggregation of fetal Tau protein in degenerating neurons in the brain of DM1 patients (Sergeant et al. 2001). The increased expression of fetal Tau isoforms results from the reduced

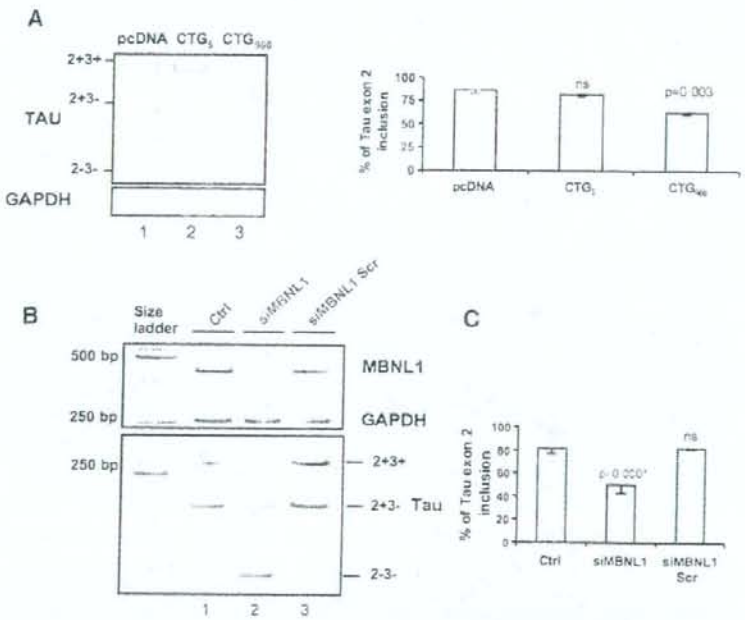

Fig. 5. Effect of long CUG repeats and loss of MBNL1 expression levels on the inclusion of Tau exon 2. A. Reduced Tau exon 2 inclusion in the presence of long CUG repeats. The proportion of Tau transcripts including exons 2 and 3 was analyzed in HeLa cells transfected with the 3′UTR of the human DMPK gene containing 5 or 960 CTG repeats, by RT-PCR. The bands were quantified and the results expressed as the percentage of transcripts including exon 2. GAPDH was used as the internal loading standard. B. Loss of MBNL1 expression reduces Tau exon 2 inclusion. An RNA duplex (siMBNL1a) against human MBNL1 (siMBNL1, lane 2) or a scrambled duplex (siMBNL1 Scr, lane 3) were used for transfection into HeLa cells. In controls (Ctrl, lane 1), the transfection agent alone was used. Note the reduced expression of MBNL1 in presence of the siMBNL1 and not of the siMBNL1 Scr (upper panel B, lane 3). RT-PCR using primers surrounding exon 2/3 were used to analyze the pattern of Tau splicing (lower panel B). Tau isoforms are indicated on the right. C. Histogram of the percentage of transcripts including exon 2. The mean and standard deviation were calculated from three individual experiments. Histograms are representative of the mean±standard deviation of three independent experiments in A and C.

inclusion of Tau exon 2/3. As shown here, MBNL1 isoform expression is also modified in the DM1 brain, raising the question of whether it is the CUG repeats or the MBNL1 fetal isoforms that are responsible for the modified splicing of Tau. To answer this question, we first analyzed the consequences of the ectopic expression of CUG repeats on the splicing of Tau in HeLa cells (Fig. 5A). Under control conditions, endogenous Tau exon 2/3 were alternately spliced in HeLa cells (Fig. 5A, lane 1). As Tau exon 3 never appears independently of exon 2, three PCR products are observed, corresponding to 2+ 3+, 2+ 3− and 2− 3− transcripts. However, the expression of CUG_{960} (Fig. 5A, lane 3), but not CUG_5 (Fig. 5A, lane 2) by HeLa cells induced a significant 25% decrease in exon 2 inclusion, demonstrating that the reduced inclusion of Tau exon 2/3 resulted from the trans-dominant effect of CUG repeats (Fig. 5A).

We next examined whether or not the loss of MBNL1 expression induced the preferential exclusion of Tau exon 2/3. Two siRNAs against human MBNL1 and two scrambled RNA

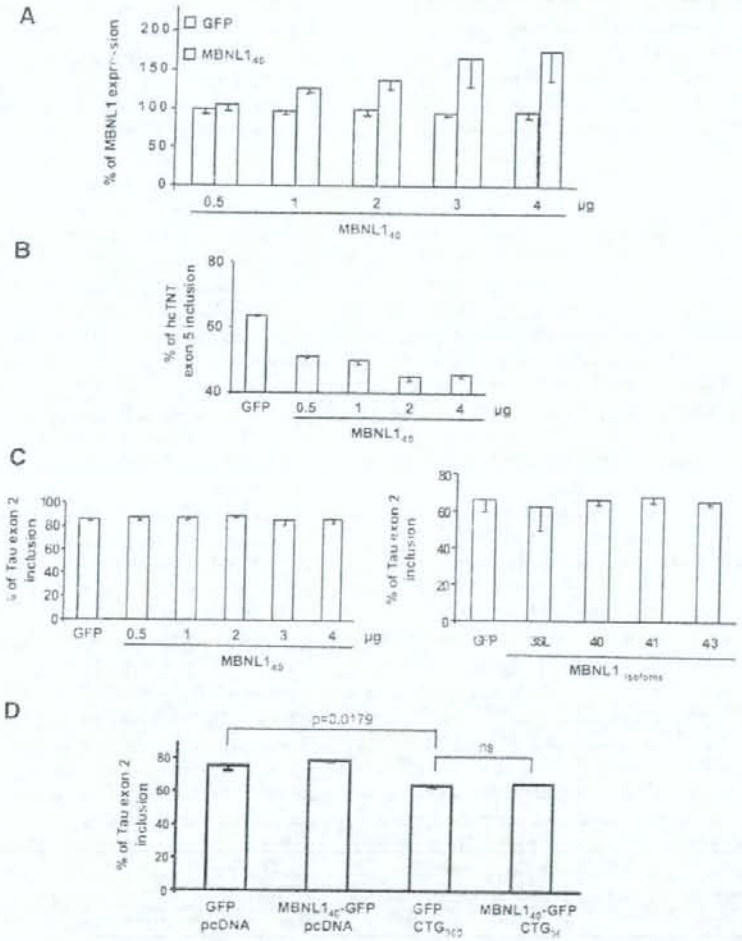

Fig. 6. Effect of MBNL1 isoforms ectopic expression on hcTNT exon 5 and Tau exon 2 splicing. A. Dose expression of $MBNL1_{40}$. A Growing quantity of $MBNL1_{40}$ plasmid (in microgram) was transfected. The amount of $MBNL1_{40}$ mRNA expressed is represented as the percentage to the control expression. A plasmid containing the GFP alone was used as a control of ectopic expression (grey bars). Note that GFP does not affect endogenous MBNL1 expression. B. Dose response exclusion of hcTNT exon 5 in presence of growing amount of MBNL1. A growing quantity of $MBNL1_{40}$ plasmid was co-transfected with hcTNT minigene. Exon 5 splicing was analyzed by RT-PCR and results are represented as the percentage of exon 5 inclusion C. Tau exon 2 inclusion is not modulated by $MBNL1_{40}$ expression nor by MBNL1 isoforms. Endegenous splicing of Tau exon 2 was analyzed after transfection of HeLa cells with an increased amount of $MBNL1_{40}$ plasmid. Two microgram of MBNL1 isoforms (36L, 40, 41 and 42) were transfected in HeLa and endogenous splicing of Tau exon 2 was analyzed by RT-PCR. The plasmid expressing GFP was used as a control. D. Tau exon 2 inclusion is unmodified by $MBNL1_{40}$ ectopic expression in presence or absence of long CUG repeats. The level of Tau exons 2 and 3 was analyzed by RT-PCR in HeLa cells transfected with the human DMPK 3′UTR containing 960 CTG repeats, in the presence of absence of cotransfection with $MBNL1_{40}$. The bands were quantified and results were expressed as percentage of transcripts that included exon 2. Histograms are representative of the mean ± standard deviation of three independent experiments in A to D.

duplexes were used (only one is shown). MBNL1 expression level (Fig. 5B, upper panel) and the splicing pattern of endogenous Tau (Fig. 5B, lower panel) were determined by RT-PCR. The MBNL1-specific RNA duplex reduced the expression level of MBNL1 mRNA (Fig. 5B, lane 2). We also observed a reduction in the expression of Tau isoforms including exon 2/3, and the increased expression of Tau isoforms lacking these exons, with this RNA duplex (Fig. 5B, lane 2), whereas the scrambled siRNA had no obvious effect on Tau splicing (Fig. 5B, lane 3). Quantitative analysis showed that the MBNL1 duplex induced a significant decrease ($p=0.0001$) in the level of exon 2 inclusion, when compared to either non-RNA controls or a scrambled RNA duplex (Fig. 5C). This decrease was not induced by an RNA duplex against β-actin (not shown). To further ascertain that the reduced inclusion of Tau exon 2 is due to the loss of MBNL1 expression, we performed a dose response effect of the loss of MBNL1 expression on Tau exon 2 splicing (supplementary Fig. 2). HeLa cells were transfected with a growing concentration of siMBNL1 duplex and endogenous MBNL1 expression and Tau exon 2 inclusion were assessed by RT-PCR. From 1 to 100 nM of duplex there was a linear decrease of MBNL1 mRNA expression (supplementary Fig. 2). In parallel, we observed a decreased percentage of Tau exon 2 inclusion from 5 to 40%, demonstrating that the reduced Tau exon 2 inclusion is in close relationship with the loss of MBNL1 expression and reproduces the splicing pattern of Tau observed in the DM1 brain.

Loss of MBNL1 function mimics DM1 phenotype and supposes that MBNL1 regulates Tau exon 2 splicing. To further address this question, a growing quantity of $MBNL1_{40}$ was expressed in HeLa cells. Fig. 6A shows that we could reach a 50% increase of MBNL1 expression by increasing the quantity of plasmid transfected. This incremental expression of MBNL1 induced a progressive decreased of hcTNT exon inclusion (Fig. 6B). The splicing of Tau exon 2 was insensitive to $MBNL1_{40}$ expression, whatever the level of expression (Fig. 6B). Moreover, none of the isoforms tested modified the splicing of Tau exon 2 (Fig. 6C) showing that splicing of Tau exon 2 is not affected by a specific isoform, as the fetal $MBNL1_{43}$ isoform. In order to investigate a recent claim that the overexpression of MBNL1 reverses the trans-dominant effect of CUG repeats by correcting for MBNL1 functional deficits (Kanadia et al., 2006), we co-transfected HeLa cells with CUG_{960} and $MBNL1_{40}$, and analyzed the endogenous splicing pattern of Tau exon 2/3. We observed that the overexpression of $MBNL1_{40}$ did not restore normal endogenous splicing of Tau to control levels (Fig. 6D).

Discussion

MBNL1 expression is central to DM1 pathophysiology, and the loss of MBNL1 function leads to the altered splicing of several transcripts in the muscle tissue of DM1 patients. Several transcripts, including those of Tau, are modified in the brain tissue of DM1 patients. However, our knowledge of MBNL1 in the human brain is limited to the fact that it is expressed at low levels (Miller et al. 2000) and is localized in the nuclear RNA foci of neocortical neurons in DM1 patients (Jiang et al., 2004). We show here that in adult human brain tissue, long MBNL1 protein isoforms, especially $MBNL1_{41}$ and/or $MBNL1_{42}$, are preferentially expressed. We characterize several transcripts and show a modification in the splicing pattern of MBNL1 in the brain tissue of DM1 patients. In addition, we show that this splicing pattern is induced by long CUG repeats, and therefore is a result of the trans-dominant effect of RNA bearing the DM1 mutation. However, this observation further adds to the complexity of the pathophysiology of DM1. For instance, the trans-dominant effect of the CUG repeats could result either from the loss of MBNL1, or from the re-expression of MBNL1 isoforms that are normally expressed early in development.

The altered splicing of MBNL1 has also been reported recently in DM1 and DM2 muscle tissue by Lin et al. (Lin et al. 2006). In the DM1 brain, in addition to the altered splicing of exon 6 seen in muscle (called exon 7 in Lin et al. (2006)), we demonstrate the preferential inclusion of MBNL1 exons 6 and 8. Moreover, we show that an increased number of MBNL1 isoforms are expressed in the DM1 brain, and that these isoforms include both exons 6 and 8, with or without exon 4. A consequence of the presence of CUG repeats is the expression of a combination of adult and fetal protein isoforms due to the trans-dominant effect. The altered splicing of MBNL1 in the human brain is consistent with the increased expression of a fetal isoform of MBNL1. MBNL1 isoforms including exons 6 and 8 are preferentially found in the fetal human brain, whereas MBNL1 isoforms lacking exon 6 are expressed in adult tissue. For instance, the predominant adult isoform is $MBNL1_{41}$.

The identification of additional MBNL1 isoforms raises the question of their cellular localization and trans-regulatory splicing properties. Are these isoforms neutralized by expanded CUG repeats? In HeLa cells, all MBNL1 isoforms in our study showed diffuse nuclear localization. However, it has previously been shown that the cellular localization of MBNL1 in COS cells is modulated by the presence or absence of exon 6 but not that of exon 8 (Lin et al. 2006). In both studies, MBNL1 isoforms were fused to GFP. However, in the present work, GFP has been placed at the N-terminus of the MBNL1 isoforms, whereas Lin et al. (Lin et al. 2006) used MBNL1 isoforms with GFP fused to the C-terminus. By transfecting GFP–MBNL1 fused constructs in COS cells, we confirm that exon 6 contributes to the nuclear localization of MBNL1. GFP position does not interfere with MBNL1 cell localization. In contrast, we show here that MBNL1 cell localization is cell-type specific as the nuclear localization of MBNL1 isoforms was not affected in HeLa. Therefore, both MBNL1 primary sequence and the cell system used should be considered to investigate MBNL1 nucleocytoplasmic shuttling. Although a difference in trans-regulatory function could not be proven using the hcTNT exon 5 splicing assay, we cannot exclude the hypothesis that MBNL1 isoforms have different trans-regulatory properties toward other targets. Therefore, the altered pattern of MBNL1 expression may contribute further to the multisystemic expression of DM1 than the mere loss of its function due to titration by CUG repeats.

In vitro experiments have suggested that the spacer between the two Zinc-finger domains is essential for the binding of MBNL1 to

CUG repeats (Kino et al. 2004). Interestingly, in our study, all the MBNL1 isoforms examined, including $MBNL1_{36L}$, which lacks the exon 4-encoded spacer between the two Zinc-finger domains, are localized to nuclear foci in the presence of long CUG repeats. Our results suggest therefore that *in vivo*, all MBNL1 isoforms, even those lacking the exon 4-encoded sequence, associate with double-stranded RNA.

In the present study, we show that the modified splicing of Tau pre-mRNAs is induced by CUG repeats, as previously observed in the DM1 brain (Sergeant et al. 2001). However, this effect only occurs with very long expansions (CUG_{960}) and not with moderate ones (CUG_{200}) (not shown). Our results are consistent with those previously shown for hcTNT exon 5, where the level of inclusion of exon 5 appears to follow CUG repeat length (Savkur et al. 2001, Philips et al., 1998). This suggests that, depending on the number of repeats, different sets of transcripts might be affected. In particular, in tissues where somatic mosaicism is important and expansion increases with age, we can hypothesize that some transcripts will only be altered at more advanced ages, leading to the late expression of specific clinical signs. This is the case in the DM1 brain, where we have previously demonstrated the importance of somatic instability; the number of CUG repeats is heterogeneous between brain regions, and very large expansions of over 4000 CUG repeats are observed (Sergeant et al., 200).

The mechanism by which CUG repeat RNAs exert their effect is thought to involve the interaction of the CUG repeats with proteins, especially the MBNL1 protein family. One possibility is that MBNL1 sequestration in foci leads to a loss of function of MBNL1 and the disrupted splicing of several target pre-mRNAs. In the present study, we show that the modified splicing of Tau pre-mRNA is induced by long CUG repeats (see also (Sergeant et al., 2001)) or by the loss of MBNL1 expression, as observed in the DM1 brain. Moreover, the reduced Tau exon 2 inclusion is dose-dependant since we showed that a growing loss of MBNL1 expression results in a growing decrease of Tau exon 2 inclusion. Conversely, incremental expression of MBNL1 or the expression of several MBNL1 isoforms does not modify the splicing pattern of Tau, whereas these isoforms and the increment expression of MBNL1 have similar trans-regulatory properties towards hcTNT exon 5 splicing. Moreover, the reduced inclusion of Tau exon 2/3 induced by the presence of long CUG repeats is not reversed by the overexpression of $MBNL1_{40}$, supporting the hypothesis that the trans-dominant effect of CUG repeats toward Tau splicing is mediated by a complete loss of MBNL1 function. A recent study demonstrated coordinated physical and functional interactions between hnRNPH, CUG-BP1 and MBNL1 in the regulation of IR splicing (Paul et al., 2006). Although the mechanism of Tau exon 2/3 splicing is currently unclear, MBNL1 could be one element of a protein complex that regulates spliceosome activity. We have recently shown that ETR-3, a member of the CELF family of splicing factors, acts as a strong repressor of Tau exon 2/3 inclusion (Leroy et al. 2006b). Other proteins potentially involved in MBNL1-mediated Tau splicing could be CUG-BP1 or hnRNPH.

A growing body of evidence, including our results, supports the hypothesis that the DM1 phenotype is in part related to a change in the splicing program due to the trans-dominant effect of CUG repeats, resulting in the mixed expression of adult and fetal isoforms of various proteins, including Tau and MBNL1. Moreover, the reactivation of fetal-like splicing machinery in adult neurons is also a concept that should be explored in the case of Tauopathies.

Acknowledgments

This work was supported by the Association Française contre les Myopathies (AFM, NM10908, NM 12126, NM 12570), INSERM, CNRS, IMPRT and Université de Lille II. Valérie Vingtdeux is a recipient of a fellowship from the Association France Alzheimer. Tom Cooper is supported by the Muscular Dystrophy Association and National Institute of Health AR.45653. Mani Mahadevan is supported by the Muscular Dystrophy Association and the US National Institute of Arthritis and Musculoskeletal and Skin Diseases. We are grateful to Martial Flactif from the Centre of Imaging of the IMPRT for his expert technical assistance with confocal microscopy. This manuscript was prepared with help from Gap Junction (www.gap-junction.com).

Appendix A. Supplementary data

Supplementary data associated with this article can be found, in the online version, at doi: 0.10.6/j.expneurol 2007 .1 020.

References

Artero, R. Prokop, A. Paricio, N. Begemann, G., Pueyo, I., Mlodzik, M. Perez-Alonso, M. Baylies, M.K., 1998. The muscleblind gene participates in the organization of Z-bands and epidermal attachments of *Drosophila* muscles and is regulated by Dmef2. Dev. Biol. 195, 131–143.

Amack, J.D., Paguio, A.P., Mahadevan, M.S., 1999. Cis and trans effects of the myotonic dystrophy (DM) mutation in a cell culture model. Hum. Mol. Genet. 8, 1975–1984.

Ashizawa, T. Dunne, C.J., Dubel, J.R., Perryman, M.B. Epstein, H.F., Boerwinkle, E. Hejtmancik, J.F. 1992. Anticipation in myotonic dystrophy. I. Statistical verification based on clinical and haplotype findings. Neurology 42, 1871–1877.

Begemann, G., Paricio, N., Artero, R., Kiss, I., Perez-Alonso, M. Mlodzik, M., 1997. Muscleblind, a gene required for photoreceptor differentiation in *Drosophila*, encodes novel nuclear Cys3His-type zinc-finger-containing proteins. Development 124, 4321–4331.

Buj-Bello, A., Furling, D., Tronchere, H., Laporte, J., Lerouge, T., Butler-Browne, G.S., Mandel, J.L., 2002. Muscle-specific alternative splicing of myotubularin-related 1 gene is impaired in DM1 muscle cells. Hum. Mol. Genet. 11, 2297–2307.

Charlet, B.N., Savkur, R.S., Singh, G., Philips, A.V., Grice, E.A. Cooper, T.A., 2002. Loss of the muscle-specific chloride channel in type 1 myotonic dystrophy due to misregulated alternative splicing. Mol. Cell 10, 45–53.

Cooper, T.A., 1998. Muscle-specific splicing of a heterologous exon mediated by a single muscle-specific splicing enhancer from the cardiac troponin T gene. Mol. Cell. Biol. 18, 4519–4525.

Fardaei, M., Rogers, M.T., Thorpe, H.M., Larkin, K., Hamshere, M.G. Harper, P.S., Brook, J.D., 2002. Three proteins, MBNL, MBLL and MBXL, co-localize *in vivo* with nuclear foci of expanded-repeat transcripts in DM1 and DM2 cells. Hum. Mol. Genet. 11, 805–814.

Harley, H.G., Brook, J.D., Rundle, S.A., Crow, S., Reardon, W. Buckler, A.J., Harper, P.S., Housman, D.E., Shaw, D.J., 1992. Expansion of an unstable DNA region and phenotypic variation in myotonic dystrophy. Nature 355, 545–546.

Harper, P.S., 1989. Myotonic Dystrophy. W.B. Saunders, Philadelphia.

Jiang, H., Mankodi, A. Swanson, M.S., Moxley, R.T., Thornton, C.A., 2004. Myotonic dystrophy type 1 is associated with nuclear foci of mutant RNA, sequestration of muscleblind proteins and deregulated alternative splicing in neurons. Hum. Mol. Genet. 13, 3079–3088.

Kanadia, R.N., Johnstone, K.A., Mankodi, A., Lungu, C., Thornton, C.A., Esson, D., Timmers, A.M., Hauswirth, W.W., Swanson, M.S., 2003. A muscleblind knockout model for myotonic dystrophy. Science 302, 1978–1980.

Kanadia, R.N., Shin, J., Yuan, Y., Beattie, S.G., Wheeler, T.M. Thornton, C.A., Swanson, M.S., 2006. Reversal of RNA missplicing and myotonin after muscleblind overexpression in a mouse poly(CUG) model for myotonic dystrophy. Proc. Natl. Acad. Sci. U. S. A. 103, 11748–11753.

Kimura, T., Nakamori, M. Lueck, J.D., Pouliquin, P., Aoike, F., Fujimura, H., Dirksen, R.T., Takahashi, M.P. Dulhunty, A.F., Sakoda, S., 2005. Altered mRNA splicing of the skeletal muscle ryanodine receptor and sarcoplasmic/endoplasmic reticulum Ca^{2+}-ATPase in myotonic dystrophy type 1. Hum. Mol. Genet. 14, 2189–2200.

Kino, Y., Mori, D., Oma, Y., Takeshita, Y., Sasagawa, N., Ishiura, S., 2004. Muscleblind protein, MBNL1/EXP, binds specifically to CHHG repeats. Hum. Mol. Genet. 13, 495–507.

Kiuchi, A., Otsuka, N., Namba, Y. Nakano, I. Tomonaga, M., 1991. Presenile appearance of abundant Alzheimer's neurofibrillary tangles without senile plaques in the brain in myotonic dystrophy. Acta Neuropathol. (Berl) 82, 1–5.

Ho, T.H., Charlet, B.N., Poulos, M.G., Singh, G. Swanson, M.S., Cooper, T.A., 2004. Muscleblind proteins regulate alternative splicing. EMBO J. 23, 3103–3112.

Ho, T.H., Savkur, R.S., Poulos, M.G., Mancini, M.A., Swanson, M.S., Cooper, T.A., 2005. Colocalization of muscleblind with RNA foci is separable from mis-regulation of alternative splicing in myotonic dystrophy. J. Cell Sci. 118, 2923–2933.

Leroy, O., Wang, J., Maurage, C.A., Parent, M., Cooper, T., Buee, L., Sergeant, N., Andreadis, A. Caillet-Boudin, M.L., 2006a. Brain-specific change in alternative splicing of Tau exon 6 in myotonic dystrophy type 1. Biochim. Biophys. Acta 1762, 460–467.

Leroy, O. Dhaenens, C.M. Schraen-Maschke, S., Belarbi, K. Delacourte, A., Andreadis, A. Sablonniere, B., Buee, L., Sergeant, N. Caillet-Boudin, M.L., 2006b. ETR-3 represses Tau exons 2/3 inclusion, a splicing event abnormally enhanced in myotonic dystrophy type 1. J. Neurosci. Res. 84, 852–859.

Lin, X., Miller, J.W., Mankodi, A., Kanadia, R.N., Yuan, Y., Moxley, R.T., Swanson, M.S., Thornton, C.A., 2006. Failure of MBNL1-dependent post-natal splicing transitions in myotonic dystrophy. Hum. Mol. Genet. 15, 2087–2097.

Mankodi, A., Urbinati, C.R., Yuan, Q.P., Moxley, R.T., Sansone, V., Krym, M., Henderson, D., Schalling, M., Swanson, M.S. Thornton, C.A., 2001. Muscleblind localizes to nuclear foci of aberrant RNA in myotonic dystrophy types 1 and 2. Hum. Mol. Genet. 10, 2165–2170.

Miller, J.W., Urbinati, C.R., Teng-Umnuay, P., Stenberg, M.G., Byrne, B.J., Thornton, C.A., Swanson, M.S., 2000. Recruitment of human muscleblind proteins to (CUG)(n) expansions associated with myotonic dystrophy. Embo J. 19, 4439–4448.

Oyamada, R., Hayashi, M., Katoh, Y. Tsuchiya, K., Mizutani, T., Tominaga, I. Kashima, H., 2006. Neurofibrillary tangles and deposition of oxidative products in the brain in cases of myotonic dystrophy. Neuropathology 26, 107–114.

Pascual, M., Vicente, M., Monferrer, L., Artero, R., 2006. The muscleblind family of proteins: an emerging class of regulators of developmentally programmed alternative splicing. Differentiation 74, 65–80.

Paul, S., Dansithong, W., Kim, D., Rossi, J., Webster, N.J., Comai, L., Reddy, S., 2006. Interaction of muscleblind, CUG-BP1 and hnRNP H proteins in DM1-associated aberrant IR splicing. Embo J. 25, 4271–4283.

Philips, A.V., Timchenko, L.T., Cooper, T.A., 1998. Disruption of splicing regulated by a CUG-binding protein in myotonic dystrophy. Science 280, 737–741.

Savkur, R.S. Philips, A.V., Cooper, T.A., 2001. Aberrant regulation of insulin receptor alternative splicing is associated with insulin resistance in myotonic dystrophy. Nat. Genet. 29, 40–47.

Sergeant, N., Sablonniere, B., Schraen-Maschke, S., Ghestem, A., Maurage, C.A., Wattez, A., Vermersch, P., Delacourte, A., 2001. Dysregulation of human brain microtubule-associated tau mRNA maturation in myotonic dystrophy type 1. Hum. Mol. Genet. 10, 2143–2155.

Taneja, K.L., McCurrach, M. Schalling, M., Housman, D. Singer, R.H., 1995. Foci of trinucleotide repeat transcripts in nuclei of myotonic dystrophy cells and tissues. J. Cell Biol. 128, 995–1002.

Vermersch, P., Sergeant, N., Ruchoux, M.M., Hofmann-Radvanyi, H. Wattez, A. Petit, H., Dwailly, P., Delacourte, A., 1996. Specific tau variants in the brains of patients with myotonic dystrophy. Neurology 47, 711–717.

Journal of Neuroscience Research 86:1994–2002 (2008)

MBNL1 Associates with YB-1 in Cytoplasmic Stress Granules

Hayato Onishi,[1] Yoshihiro Kino,[1,2] Tomoko Morita,[1] Eugene Futai,[1] Noboru Sasagawa,[1] and Shoichi Ishiura[1]*

[1]Department of Life Sciences, Graduate School of Arts and Sciences, University of Tokyo, Tokyo, Japan
[2]Laboratory for Structural Neuropathology, Brain Science Institute, RIKEN, Tokyo, Japan

The muscleblind-like (MBNL) protein family is thought to be involved in the molecular mechanism of myotonic dystrophy (DM). Although it has been shown to have splicing activity, a broader function in cellular RNA metabolism has been implicated. In this study, we attempted to find the binding proteins of MBNL1 in order to elucidate its physiological function. First, we performed a GST pull-down assay using GST-MBNL1-6xHis as bait. Several proteins were identified, including YB-1, a multifunctional DNA/RNA-binding protein, and DDX1, a DEAD box RNA helicase. MBNL1 formed an RNP complex with YB-1 and DDX1 in binding assays. YB-1 also showed a weak but significant effect on α-actinin splice site selection. Interestingly, in response to stress, MBNL1 moved to cytoplasmic stress granules, where it colocalized with YB-1, which was previously reported to be a component of stress granules. We found that DDX1 also colocalized with MBNL1 at stress granules. These results provide new insight into the dynamics of MBNL1 in response to stress, and they suggest a role for MBNL1 in mRNA metabolism in the cytoplasm.

Key words: myotonic dystrophy; MBNL1; YB-1; stress granules; splicing

Myotonic dystrophy (dystrophia myotonica; DM) is one of the most common human muscular dystrophies, occurring at a frequency of 1 in 8,000 (Harper, 2001). The clinical features of DM include myotonia, cataracts, insulin resistance, and cognitive dysfunction (Meola et al., 2003). DM is an autosomally inherited disorder that is classified into two types, DM1 and DM2, based on the expansion of tri (CTG)- and tetra (CCTG)-nucleotide repeats in the 3′-UTR of *DMPK* (Brook et al., 1992; Mahadevan et al., 1992; Fu et al., 1993) and intron 1 of *ZNF9* (Liquori et al., 2001), respectively. DM1 and DM2 have similar phenotypes even though they are caused by unrelated mutations (Day et al., 2003). Various hypotheses have been proposed to explain how untranslated mutations can lead to a dominant pathogenic phenotype; however, several lines of evidence support a "gain-of-function" model for expanded RNA repeats. No DMPK mutation except for the repeat expansion has ever been reported, indicating that loss of function of DMPK is not the major cause of DM1. Although mice deficient in DMPK show mild myopathy and abnormalities in cardiac conductance, they do not reproduce other symptoms of DM1 (Jansen et al., 1996; Reddy et al., 1996; Berul et al., 1999). On the other hand, mice expressing expanded CUG repeats inserted in the 3′-UTR of the muscle-specific actin gene developed myotonia and DM-like myopathy (Mankodi et al., 2000). There are several reports that CUG or CCUG repeat RNAs form nuclear foci in cells or tissues of DM1 or DM2 patients and mice expressing expanded CUG repeats by using fluorescent in situ hybridization (FISH; Taneja et al., 1995; Davis et al., 1997; Amack et al., 1999; Mankodi et al., 2000, 2001; Liquori et al., 2001). This evidence suggests that the expressions of expanded CUG or CCUG repeats are likely to be central features and sufficient for causing these symptoms.

The RNA repeat foci seem to sequester several RNA binding proteins, such as those of the well-known MBNL family (Fardaei et al., 2001, 2002; Mankodi et al., 2001). MBNL1, which has four Cys_3His zinc-finger domains, is a human homologue of *Drosophila* muscleblind (Begemann et al., 1997), which has been reported to play some role in the differentiation of eye and muscle (Begemann et al., 1997; Artero et al., 1998). MBNL1 was first isolated as a CUG repeat binding protein in relation to DM (Miller et al., 2000). Previously, the binding specificity of MBNL1 was characterized, and target RNA sequence was determined (Kino et al., 2004). The MBNLs have been established as regulators of alternative splicing (Ho et al., 2004). Recently, it was

Supplementary Material for this article is available online at http://www.mrw.interscience.wiley.com/suppmat/0360-4012/suppmat/ (www.interscience.wiley.com).

Contract grant sponsor: Ministry of Health, Labor and Welfare, Japan; Contract grant sponsor: HFSP.

*Correspondence to: Shoichi Ishiura, Department of Life Sciences, Graduate School of Arts and Sciences, University of Tokyo, Tokyo, Japan. E-mail: cishiura@mail.ecc.u-tokyo.ac.jp

Received 2 October 2007; Revised 30 November 2007; Accepted 17 December 2007

Published online 11 March 2008 in Wiley InterScience (www.interscience.wiley.com). DOI: 10.1002/jnr.21655

suggested that *Muscleblind* has a role in translational control through a modulation of RNA stability in the cytoplasm (Houseley et al., 2005). In addition, it was shown that localized expression of the integrin α3 is regulated at the level of RNA localization by MBNL2 (MLP1), a human paralogue of MBNL1 (Adereth et al., 2005). These findings imply that MBNL1 might also have a similar role in mRNA metabolism in the cytoplasm. The physiological functions of MBNL1 are largely unknown except that it has splicing activity and its function is down-regulated in DM. Although therapeutic strategies that restore MBNL1 function to normal would likely benefit those with DM, a broader understanding of MBNL1 function is important for elucidating DM pathogenesis.

MATERIALS AND METHODS

Plasmid Construction

The open reading frames for *YB-1*, *DDX1*, *TIA-1*, and *DCP2* were amplified by PCR from a human skeletal muscle cDNA library (Clontech, Logan, UT) and cloned into pcDNA3.1-V5 (Invitrogen, Carlsbad, CA), pECFP-C1 (Clontech), or pcDNA3-HA (Invitrogen) using conventional molecular biological techniques. $MBNL1_{40}$ was cloned into pEGFP-N1 (Clontech) or pSecDk. The pSecDk vector was generated by deleting the IgG sequence from pSecTagA (Invitrogen). The EF1-EF2 region of α-actinin was amplified by PCR from rat genome DNA and cloned into the BglII-SalI site of pEGFP-C1 (Clontech). The nucleotide sequences of the DNA inserts were confirmed by sequencing.

Antibodies

Anti-MBNL1 rabbit polyclonal antibodies were raised using bacterially expressed $MBNL1_{40}$-6xHis as the antigen. The serum was purified with $MBNL1_{40}$-coupled Affigel 10 (Bio-Rad, Hercules, CA) and cleared by GST-6xHis-bound glutathione Separose (Amersham, Arlington Heights, IL). Goat anti-TIA-1 was purchased from Santa Cruz Biotechnology (Santa Cruz, CA). Rat anti-HA 3F10 was purchased from Roche (Indianapolis, IN). Mouse anti-V5 and anti-myc antibodies were purchased from Invitrogen. Alexa Fluor 568-labeled goat anti-mouse IgG, Alexa Fluor 488-labeled donkey anti-rabbit IgG, Alexa Fluor 546-labeled donkey anti-goat IgG, and Alexa Fluor 488-labeled donkey anti-rat IgG were purchased from Molecular Probes (Eugene, OR).

Protein Purification

Recombinant GST-$MBNL1_{40}$-6xHis was expressed in bacteria and purified as described elsewhrere (Kino et al., 2004). Briefly, pET-GX containing $MBNL1_{40}$ was transformed into BL21 (DE3) cells and cultured overnight in LB medium. The culture was then diluted and shaken at 37°C for 1.5 hr, or until the OD_{600} reached 0.3–0.4, and then 0.2 mM IPTG was added. During induction, the culture was shaken at 25°C for 4 hr. The bacterial cells were then collected and lysed twice in a French pressure cell press (Ohtake Works, Co.) before being centrifuged at 5,000*g* for 20 min. The supernatant was subjected to affinity purification using glutathione Sepharose 4B (Amersham Biosciences). The beads were washed with ATP $MgSO_4$ buffer to exclude DnaK, and GST-$MBNL1_{40}$-6xHis was eluted with 50 mM Tris-HCl, pH 8.8, and 10 mM glutathione (reduced type). The eluate was then mixed with NaCl and imidazole before the addition of Talon Metal Affinity Resin (Clontech) according to the manufacturer's protocol. Finally, the purified proteins were dialyzed against a stock buffer (50 mM Tris-HCl, pH 8.0, 100 mM NaCl, and 2 mM 2-mercaptoethanol). The quantity and purity of the samples were checked by SDS-PAGE with Coomassie brilliant blue (CBB) staining. The identity of GST-$MBNL1_{40}$-6xHis was confirmed by peptide mass fingerprinting with mass spectrometry (AXIMA-CFR; Shimadzu) following digestion with trypsin.

GST Pull-Down Assay

Mouse muscle and heart (2 g each) were homogenized in lysis buffer (50 mM Tris-HCl, pH 8.0, 100 mM NaCl, 2 mM 2-mercaptoethanol, 0.5% NP-40, 0.5% Triton X-100, and 1/1,000 vol protease inhibitors) using a Hitachi homogenizer and centrifuged at 15,000*g* for 20 min. Next, the supernatant was precleared with 500 μl of glutathione Sepharose for 2 hr and with GST-6xHis-bound glutathione Sepharose for 2 hr at 4°C. Finally, the supernatant was mixed with 20 μg of GST-$MBNL1_{40}$-6xHis and rotated overnight at 4°C. The beads were washed five times with lysis buffer, and the complex was eluted by cleavage with 3 U thrombin for 1 hr at 20°C, then subjected to SDS-PAGE.

In-Gel Trypsin Digestion and Analysis by Matrix-Assisted Laser Desorption/Ionization Tandem Time-of-Flight (MALDI-TOF/TOF) Mass Spectrometry

Pull-down assays were performed as described above. The bound proteins were separated by 12.5% SDS-PAGE and stained with Silver Quest (Invitrogen). The bands were excised from the gel and destained, dehydrated with acetonitrile for 10 min, and dried completely under a vacuum pump for 10 min. Each band was placed in 20 μl of 5 mM NH_4HCO_3 containing 1 pmol sequencing-grade trypsin (Promega, Madison,WI) at 37°C overnight. Aliquots of the trypsinized samples were analyzed by nanoliquid chromatography and automatically spotted with alfa-cyano-4-hydroxyl-cinnamic acid solution on a stainless-steel target and air dried. MALDI-TOF/TOF analysis was conducted with a Proteomics analyzer 4700 (Applied Biosystem, Foster City, CA). The proteins were identified by database searches on the web with Mascot (Matrix Science, Ltd., London, United Kingdom).

Western Blotting

The samples were subjected to 10% SDS-PAGE and transferred to PVDF membranes (Immobilon-P; Millipore, Bedford, MA). The membranes were then blocked with 5% skim milk in TPBS (0.05% Tween 20 in PBS) for 1 hr at room temperature and incubated with primary antibodies in TPBS. After washing, the membranes were incubated for 1 hr with horseradish peroxidase (HRP)-conjugated secondary antibodies. The immunoreactive bands were visualized with the LAS-3000 imaging system (Fujifilm, Tokyo, Japan).

Immunoprecipitation

COS-7 cells were transfected with myc-tagged constructs of MBNL1 and V5-tagged constructs of YB-1 or DDX1 using FuGENE6 (Roche, Basel, Switzerland). Cells from two 10-cm plates were homogenized in 500 μl lysis buffer [50 mM Tris-HCl, pH 8.0, 150 mM NaCl, 5 mM dithiothreitol (DTT), 1 mM EDTA, 1% (w/v) Triton X-100, and protease inhibitor cocktail]. The lysates were then centrifuged at 100,000*g* for 15 min at 4°C. The supernatant was precleared with protein G Sepharose 4 fast flow beads (Amersham Biosciences, Piscataway, NJ) for 1 hr and then incubated with anti-V5 antibodies fixed on beads. After the beads were washed five times with lysis buffer, the precipitates were analyzed by SDS-PAGE and immunoblotted with either anti-myc or anti-V5 antibodies.

Immunocytochemistry and Image Analysis

HeLa and COS-7 cells were fixed with PBS containing 4% (w/v) paraformaldehyde for 15 min and permeabilized with 0.1% (w/v) Triton X-100 in PBS for 15 min. After the buffer was exchanged for 3% (w/v) BSA in PBS, the cells were incubated with the first antibody in 3% BSA in PBS for 1 hr, washed with PBS, and then incubated with the second antibody in 3% BSA in PBS for 1 hr. After washing with PBS, the samples were embedded in Mowiol (Calbiochem, La Jolla, CA). Cell images were acquired on a Zeiss LSM510 Meta laser scanning confocal microscope (Carl Zeiss, Jena, Germany) or IX70 microscope (Olympus, Tokyo, Japan).

Polysome Analysis

HeLa (10-cm dish) cells were exposed to 50 μg/ml cycloheximide at 37°C for 10 min, washed twice with cold PBS, and resuspended in 300 μl TKM buffer (10 mM Tris-HCl, pH 7.5, 100 mM KCl, 5 mM $MgCl_2$, and 50 μg/ml cycloheximide). The cells were then homogenized by passing them through a 27-gauge needle 10 times. Both the PBS and the TKM contained 50 μg/ml cycloheximide. The homogenate was centrifuged at 2,000*g* for 10 min at 4°C, and the supernatant was then loaded onto a gradient of 15–40% (w/v) sucrose in TKM and sedimented for 60 min at 4°C at 40,000 rpm (18 kG) in a swinging bucket rotor. The gradient was collected in 15 fractions, with concomitant measurement of the absorbance at 254 nm. The proteins were precipitated with trichloroacetic acid and subjected to SDS-PAGE and Western blot analysis, as described above.

Splicing Assays

For the in vivo splicing assays, HEK293 cells were plated in 3.5-cm or 6-cm dishes and cultured for 24 hr in DMEM plus 10% FBS before plasmid transfection. Cells were grown to 60–80% confluence and then transiently cotransfected using FuGENE 6 (Roche) according to the manufacturer's instructions with 300 ng splicing reporter and 4 μg YB-1-V5, MBNL1-myc, or DDX1-V5. The cells were collected after 48 hr, total RNA was extracted using an RNeasy Kit (Qiagen, Valencia, CA), and the samples were analyzed by RT-PCR. Reverse-transcription was done by using PrimeScript Reverse Transcriptase (TaKaRa). Spliced products were amplified using EGFP primer (Fw: CATGGTCCTGCTGGAGTTCGTG, Rv: GTTTCAGGTTCAGGGGGAGGTGTG) and separated by 6% polyacrylamide gel.

RESULTS

Pull-Down Screening of MBNL1

MBNL1 has nine splicing isoforms (Kino et al., 2004; Pascual et al., 2006). The ratio of each isoform is likely to change during development and differentiation of muscle (Kanadia et al., 2006). Recently, it was shown that MBNL2 (MLP1) is involved in the local translation of the integrin α3 by transporting the transcript to specific points in the cytoplasm (Adereth et al., 2005). Therefore, we focused on both the nuclear and the cytosolic compartment of MBNL1, and we selected $MBNL1_{40}$, which localizes to both compartments, for use as bait in a GST pull-down assay. Double-tagged GST-MBNL1-6xHis was purified in a two-step procedure. Purified GST-MBNL1-6xHis was bound to glutathione beads and mixed with a mouse muscle or heart lysate. After incubation overnight, the beads were washed extensively, and the proteins were eluted by thrombin cleavage. After elution, the complexes in the experimental and control samples were compared by SDS-PAGE (Fig. 1). About 20 bands were detected in the sample containing muscle lysate as prey. Each band was excised from the gel and digested with trypsin. The trypsinized peptides were then subjected to MADLI-TOF/TOF analysis, and each protein was identified in MASCOT software (Suppl. Table I). Seven proteins among 20 bands were identified, and these were YB-1, DDX1, phenylalaninyl-tRNA synthetase α and β subunits, amylo-1,6-glucosidase, and several small and large ribosomal subunits. YB-1 is a multifunctional RNA/DNA binding protein and has a role in transcriptional and posttranscriptional RNA metabolism, including splicing (Stickeler et al., 2001; Rapp et al., 2002; Kohno et al., 2003; Raffetseder et al., 2003; Allemand et al., 2007). DDX1 is part of the DEAD box RNA helicase family (Cordin et al., 2006). From all of the proteins identified, we focused our attention on the two proteins known to be involved in mRNA metabolism.

Interactions Between MBNL1 and YB1 or DDX1

To confirm the interaction between MBNL1 and YB-1 or DDX1, we performed a pull-down assay. Forty-eight hours after transfection with YB-1-V5 or DDX1-V5, each COS-7 lysate was mixed with GST-$MBNL1_{40}$-6xHis bound to glutathione Sepharose. After 4 hr, the beads were washed thoroughly and boiled in SDS sample buffer. The binding of these proteins was confirmed (Fig. 2A). As negative controls, RNA binding proteins HuR and calreticulin were shown not to bind MBNL1 (data not shown). Next, immunoprecipitation (IP) assays were performed against MBNL1-myc and YB-1-V5 expressed in COS-7 (Fig. 2B). MBNL1-myc

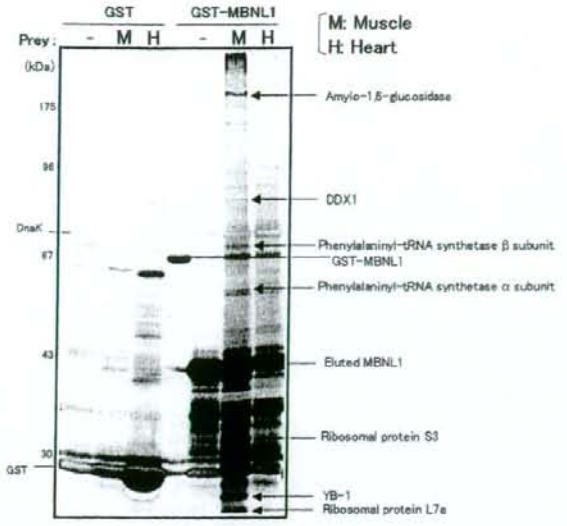

Fig. 1. GST pull-down assay with $MBNL1_{40}$. Identification of $MBNL1_{40}$-interacting proteins by pull-down assay and mass spectrometry. GST-$MBNL1_{40}$-6xHis (20 μg) or GST-6xHis (20 μg) was incubated for 16 hr with 2 g mouse muscle (M) or heart (H) lysate. The MBNL1 complex was eluted by thrombin cleavage. Twenty bands that were reproducibly observed in the GST-$MBNL1_{40}$-6xHis pull-down with muscle were subjected to MALDI-TOF/TOF analysis and identified as indicated. Accession Nos. are as follows: amylo-1,6-glucosidase, XM_131166.8; DEAD (Asp-Glu-Ala-Asp) Box polypeptide 1, NM_134040.1; phenylalanyl-tRNA synthetase α subunit, NM_011811.3; phenylalanyl-tRNA synthetase β subunit, NM_025648.2; ribosomal protein S3, NM_012052.2; Y-box transcription factor, NM_011732; and ribosomal protein L7a, NM_013721.3.

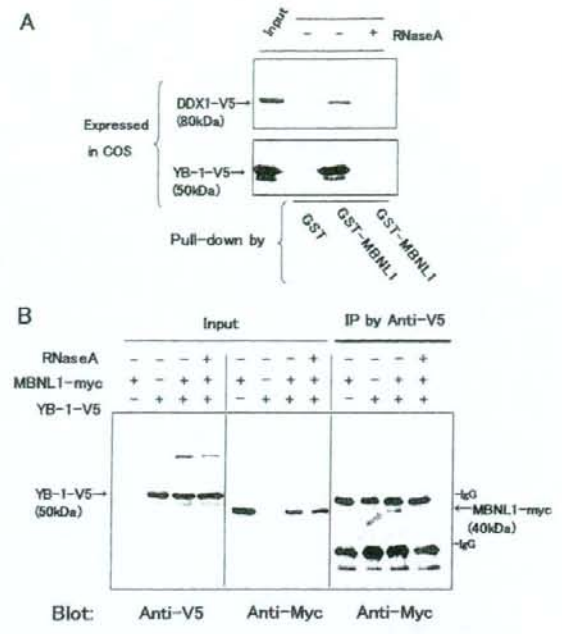

Fig. 2. Interactions of MBNL1 with YB1 or DDX1. **A:** Pull-down assays were performed with GST-$MBNL1_{40}$-6xHis as bait. In the upper panel, transiently expressed DDX1- or YB-1-V5 was pulled-down by GST-$MBNL1_{40}$-6xHis. Binding was diminished by the addition of RNase A. **B:** Immunoprecipitation (IP) was performed using COS-7 cells transiently transfected with $MBNL1_{40}$-myc and YB-1-V5. As indicated by an arrow, MBNL1-myc was present in the YB-1-V5 complex precipitated by anti-V5 antibody. When an RNase A-containing lysis buffer was used, the MBNL1 band was diminished.

was specifically coimmunoprecipitated with YB-1-V5 by anti-V5 antibody. Because these associations diminished when the lysates were pretreated with RNase A (Fig. 2B), it was suggested that these proteins are assembled into RNPs on an RNA scaffold.

α-Actinin Minigene Splicing Assay

Previously, YB-1 was shown to interact with MeCP2 through RNA and to mediate the alternative splicing of CD44 (Young et al., 2005). To investigate the functional interaction between MBNL1 and YB-1, we tested the splicing activity of YB-1 on one of the targets of MBNL1, the α-actinin minigene (Vicente et al., 2007). HEK293 cells were transfected with the minigene and each effector protein plasmid. RT-PCR analysis showed that YB-1 promoted exon skipping, as did MBNL1, although the response was weaker (Fig. 3). It suggests that MBNL1 and YB-1 may cooperate in the alternative splicing of α-actinin. The effect of DDX1 was not significant. We also determined the splicing activity of YB-1 and DDX1 on Clcn1 minigene, but no significant change was observed (data not shown).

Colocalization of MBNL1, YB-1, DDX1, and TIA-1 in HeLa Cells

Although YB-1 affected the splicing of α-actinin, the effect was weak. Combining this with the fact that some ribosomal proteins were identified as MBNL1-binding proteins (Fig. 1), we speculate that the interaction between MBNL1 and YB-1 occurs in the cytoplasm rather than in the nucleus. YB-1 is one of the components of mRNA processing bodies (P-bodies) and stress granules (SGs; Goodier et al., 2007; Yang and Bloch, 2007). Considering that MBNL1 also functions in mRNA metabolism in the cytoplasm, we investigated the localization of GFP-MBNL1 or MBNL1-myc, YB-1-V5, and DDX1-V5 in HeLa cells (Fig. 4). Under normal conditions, MBNL1 and DDX1 localized mainly to the nucleus. On the other hand, nuclear localization of YB-1 was weak. When HeLa cells were subjected to arsenite stress, MBNL1 and YB-1 or DDX1 strongly colocalized to SGs (Fig. 4A,B). CFP-tagged TIA-1, a SGs marker, also colocalized with MBNL1 in SGs (Fig. 4C).

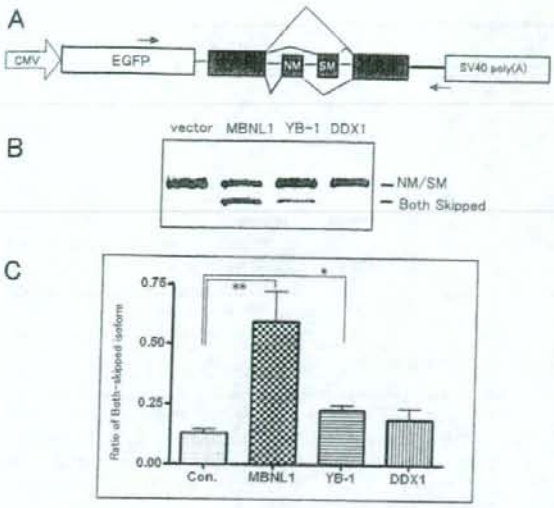

Fig. 3. Splicing of α-actinin by MBNL1. **A:** Diagram of the α-actinin minigene. The sequence of α-actinin containing NM (non-muscle) and SM (smooth muscle) alternative exons was inserted into the ORF of EGFP-C1. **B:** Upper band indicates NM- or SM-including isoform. Lower band indicates both skipped isoforms. **C:** Quantification of the ratio of both-skipped isoform. When transfected with $MBNL1_{40}$-myc, the both-skipped isoform was promoted. YB-1-V5 also up-regulated the isoform, although less than MBNL1. DDX1-V5 did not significantly affect the splicing. The results are expressed as the mean ± SD of four independent experiments. $*P < 0.05$, $**P < 0.01$.

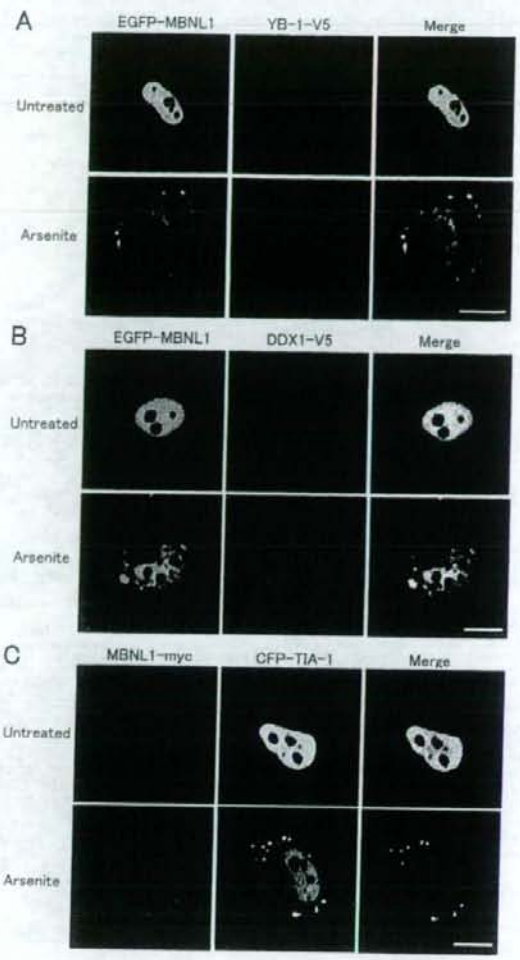

Fig. 4. Colocalization of MBNL1 and YB-1/DDX1 in HeLa. HeLa cells were cotransfected with each pair of expression plasmids. The cells were treated with sodium arsenite (0.5 mM, 45 min) 24 hr after transfection. Cell images were obtained by confocal microscopy. **A:** EGFP-MBNL1 and YB-1-V5 colocalized at cytosolic granules. **B:** DDX1-V5 colocalized with EGFP-MBNL1, as did YB-1-V5. **C:** MBNL1-myc and CFP-TIA-1 were also colocalized, as in A and B. Scale bars = 10 μm.

Production of MBNL1 Polyclonal Antibody and Endogeneous Localization of MBNL1

To investigate the cellular localization of MBNL1, we raised polyclonal antibodies against $MBNL1_{40}$ and observed endogenous MBNL1 localization. The specificity of the antibodies was confirmed by Western blotting (Fig. 5A). Next, using these antibodies, endogenous MBNL1 localization was investigated in COS-7 cells (Fig. 5). Under normal conditions, endogeneous MBNL1 localized mainly to the nucleus. After arsenite treatment, MBNL1 moved to cytoplasmic granules in the cytoplasm and strongly colocalized with TIA-1. It should be noted that MBNL1 also localized to SGs in response to heat stress in HeLa cells as well as in C2C12 myoblasts (data not shown). Therefore, the SG localization of MBNL1 would be a universal phenomenon and should have some physiological functions in SGs.

To examine whether MBNL1 localizes to SGs specifically, we subsequently examined the colocalization of MBNL1 and DCP2, a P-bodies marker. In COS-7 cells transfected with MBNL1-myc and HA-DCP2, colocalization in P-bodies was not detected in response to arsenite stress as well as in normal conditions (Fig. 5B). Thus, we concluded that the MBNL1 granules are mainly SGs, but the possibility that the MBNL1 granules partially overlap with P-bodies cannot be excluded.

YB-1 but Not MBNL1 Associates With Polysomes

Several lines of evidence suggest that YB-1 associates with polysomes (Miwa et al., 2006; Nashchekin et al., 2006). Thus, to investigate further the interaction of MBNL1 and YB-1 in cytoplasmic mRNPs, we per-

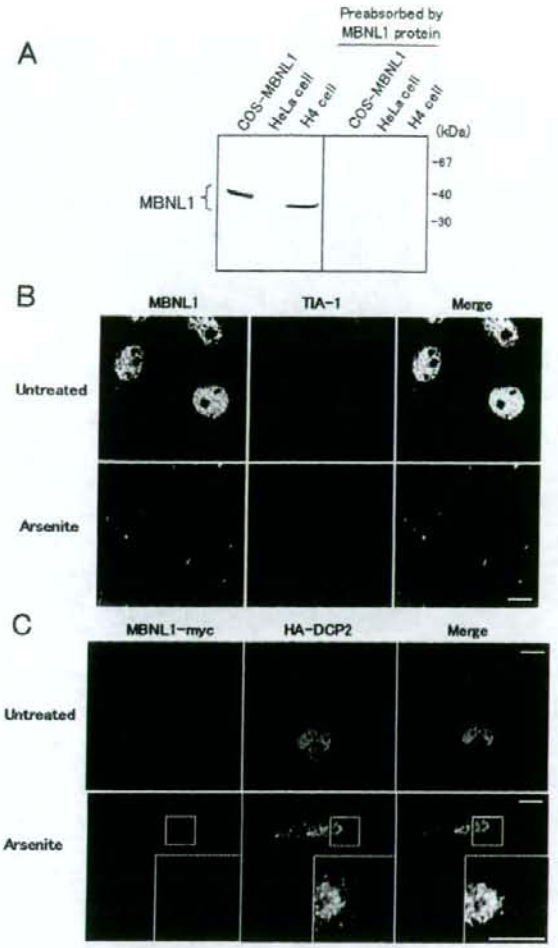

Fig. 5. Endogenous MBNL1 granules in COS-7 cells. **A:** Specificity of polyclonal antibody against MBNL1. Overexpressed $MBNL1_{40}$-myc has a higher molecular weight than that of endogeneous MBNL1 in HeLa or H4 cells. Preabsorption by $MBNL1_{40}$ entirely abolished the staining. **B:** MBNL1 and TIA-1 colocalize endogenously at stress granules after arsenite stress. **C:** MBNL1 granules are distinct from P-bodies. $MBNL1_{40}$-myc and HA-DCP2 were cotransfected into COS-7 cells. The cells were treated with 0.5 mM arsenite for 45 min. Each of the granule types appeared in distinct locations. The MBNL1 granules are larger than those of DCP2. Scale bars = 10 μm.

formed sucrose gradient fractionation. Although YB-1 was found to associate with polysomes, endogenous MBNL1 was not (Fig. 6). Consistent with this result, transiently transfected MBNL1-myc did not associate with polysomes. This suggests that MBNL1 associates with smaller mRNP particles. Our results for MBNL1 are similar to those for Smaug, an mRNA-binding protein that forms SGs like cytoplasmic foci (Baez and Boccaccio 2005). At these foci, Smaug is said to repress the translation of mRNAs. Because YB-1 cofractionated with MBNL1, the interaction of the two proteins may occur in small mRNPs, not in polysomes.

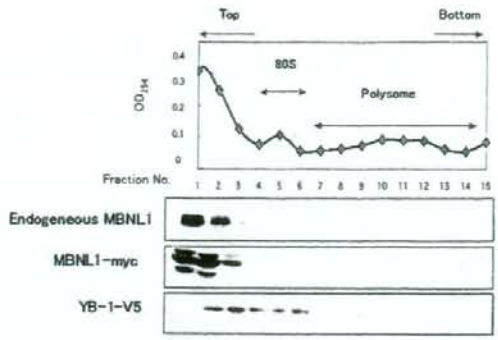

Fig. 6. Polysome analysis. Extracts of HeLa cells that had been incubated with cycloheximide were sedimented through sucrose gradients as described. The polysome and 80S single ribosome sedimentation profiles are shown by A_{254} absorbance. Western blot analysis showed that endogenous MBNL1 was present exclusively in the lighter fractions (lanes 2, 3). YB-1 was present in a broad manner in polysome fractions.

DISCUSSION

The initial aim of this study was to identify MBNL1-binding proteins. We identified several MBNL1-interacting proteins by pull-down and mass spectrometric analyses and subsequently investigated the interaction of MBNL1 with YB-1 and DDX1. YB-1, human Y-box binding protein, belongs to a family of multifunctional nucleic acid-binding proteins. Y-box proteins contain a cold-shock domain (CSD), which is highly conserved, and function as RNA chaperones. YB-1 appears to have roles in RNA splicing (Raffetseder et al., 2003; Young et al., 2005) and translation (Pascual et al., 2006), DNA repair, and transcription (Chernukhin et al., 2000; Klenova et al., 2004; Roberts et al., 2007). Thus, it regulates gene expression at both the transcriptional and the posttranscriptional levels (Pascual et al., 2006).

During the course of our analysis of the interaction between MBNL1 and YB-1, we found that MBNL1 forms SGs in the cytoplasm, like YB-1. Our immunoprecipitation results confirmed that the interaction was mediated by RNA molecules. The two proteins cofractionated in small RNP fractions rather than as polysomes. This suggests that they may form RNP complexes before the bound mRNAs are transported to actively translating ribosomes. We also examined the functional interaction between MBNL1 and YB-1 using an α-actinin minigene splicing assay, and we found that YB-1 weakly promoted SM/NM exon skipping, like MBNL1. Recent reports have described the function of YB-1 in RNA splicing. It

is therefore possible that MBNL1 and YB-1 function cooperatively during splicing.

The DEAD box RNA helicase family is also implicated in RNA splicing (Miller et al., 2000). Although in our system the contribution of DDX1 to alternative splicing could not be detected, it is possible that DDX1 affects the splicing activity of MBNL1 toward other targets. Micro-RNAs (miRNA) are increasingly recognized as major regulators of gene expression in eukaryotes, and DDX1 was recently identified as one of the components of the microprocessor complex (Gregory et al., 2004). It is intriguing to speculate that MBNL1 is also functionally related to miRNA biogenesis. Additionally, DDX1 was demonstrated to associate with cleavage stimulation factor and to be involved in processing the 3′-ends of pre-mRNA molecules (Bleoo et al., 2001). It is possible that MBNL1 is also part of the cleavage body in the nucleus, where it may play a role in constitutive RNA metabolism.

In our study, MBNL1, YB-1, and DDX1 were found to colocalize in the cytoplasm rather than in the nucleus in response to stress. A distinct feature of MBNL1 was its presence in cytosolic foci, and we demonstrated that MBNL1 colocalized with YB-1, DDX1, and TIA-1 at apparent SGs. SGs are discrete cytoplasmic aggregates that can be induced by a variety of stresses, including heat shock, hypoxia, oxidative stress, and viral infections (Anderson and Kedersha, 2002). SGs are considered to be sites of mRNA triage that regulate mRNA stability and translatability. The accumulation of RNAs into dense globules could keep them from reacting with harmful chemicals and safeguard the information that they encode. Molecules can go down one of three paths: storage, degradation, or reinitiation of translation. Recently, it was reported that YB-1, in association with the antiretroviral factor APOBEC3G, relocalizes from P-bodies to SGs when cells are exposed to heat shock stress. Our results show that MBNL1 granules are distinct from P-bodies but that sometimes they are located adjacent to one another. Considering these facts, when a cell is subjected to arsenite stress, YB-1 and MBNL1 colocalized in SGs. Our pull-down screen was not specific for stress conditions; thus, YB-1 and MBNL1 should also interact under normal physiological conditions. Supporting this, the interaction was observed in a nonstressed condition (Fig. 2). Among the proteins identified in our primary screen, the ribosomal protein L7a was identified as a component of SGs (Kim et al., 2006). The ribosomal protein S3 is also a component of SGs (Kedersha et al., 2002). Thus, four of the seven proteins identified in our screen are SGs-related proteins, which strongly suggests that MBNL1 is physiologically related to SGs. Because not all of the ribosomal proteins localized to SGs (e.g., L5 and L37), the components of SGs should be further studied. Investigations of the other MBNL1-interacting proteins as candidate SGs components, such as phenylalaninyl-tRNA synthetase subunits α and β and amylo-1,6-glucosidase, would also be interesting.

The expression of most genes is regulated by multiple mechanisms, and an important control of gene expression is exerted through mRNA stability. The stability of mRNAs is regulated by a variety of signals acting on specific sequences within the RNA. Previously, muscleblind was suggested to play a role in RNA stability in the cytoplasm in *Drosophila* (Houseley et al., 2005). Our data about cytoplasmic dynamics of MBNL1 might support this novel function of muscleblind. In addition, TTP, one of the C_3H zinc finger protein same as muscleblind, was shown either to promote AU-rich element (ARE)-RNA degradation or increase their stability (Houseley et al., 2005). Because TTP is one of the most related genes to MBNL1 in the point of its domain structure, it is reasonable to assume that MBNL1 also has a function in affecting the stability of mRNA in the cytoplasm. Target RNA sequence of MBNL1 is likely to be CHHG (H is A, U, or C) motif (Kino et al., 2004). Because every mRNA should have each specific sequence in 3′-UTR, it is possible that MBNL1 binds to mRNAs, which has a CHHG motif in the 3′-UTR, and controls their RNA stability.

Recently, for the RNA-binding motif protein 4 (RBM4), which plays a regulatory role in alternative splicing of precursor mRNA, it was demonstrated that its functions in translation control are modulated by cell stress (Lin et al., 2007). Although the relation and dynamics between splicing activity and translation control are unknown, it is intriguing to assume that these splicing regulators, including MBNL1, dynamically shuttle between nucleus and cytoplasm in response to cell stress. Further investigation should be done to clarify these splicing regulators dynamics.

In summary, our study demonstrates that MBNL1 formed cytoplasmic SGs and colocalized with YB-1 and DDX1. The functional significance of these events should be investigated further and may lead to a better understanding of the pathogenesis of DM.

ACKNOWLEDGMENTS

We thank Dr. S. Imajoh-Ohmi for mass spectrometry analysis.

REFERENCES

Adereth Y, Dammai V, Kose N, Li R, Hsu T. 2005. RNA-dependent integrin alpha3 protein localization regulated by the Muscleblind-like protein MLP1. Nat Cell Biol 7:1240–1247.

Allemand E, Hastings ML, Murray MV, Myers MP, Krainer AR. 2007. Alternative splicing regulation by interaction of phosphatase PP2Cgamma with nucleic acid-binding protein YB-1. Nat Struct Mol Biol 14:630–638.

Amack JD, Paguio AP, Mahadevan MS. 1999. Cis and trans effects of the myotonic dystrophy (DM) mutation in a cell culture model. Hum Mol Genet 8:1975–1984.

Anderson P, Kedersha N. 2002. Stressful initiations. J Cell Sci 115:3227–3234.

Artero R, Prokop A, Paricio N, Begemann G, Pueyo I, Mlodzik M, Perez-Alonso M, Baylies MK. 1998. The muscleblind gene participates

in the organization of Z-bands and epidermal attachments of *Drosophila* muscles and is regulated by Dmef2. Dev Biol 195:131–143.

Baez MV, Boccaccio GL. 2005. Mammalian Smaug is a translational repressor that forms cytoplasmic foci similar to stress granules. J Biol Chem 280:43131–43140.

Begemann G, Paricio N, Artero R, Kiss I, Perez-Alonso M, Mlodzik M. 1997. *Muscleblind*, a gene required for photoreceptor differentiation in *Drosophila*, encodes novel nuclear Cys_3His-type zinc-finger-containing proteins. Development 124:4321–4331.

Berul CI, Maguire CT, Aronovitz MJ, Greenwood J, Miller C, Gehrmann J, Housman D, Mendelsohn ME, Reddy S. 1999. DMPK dosage alterations result in atrioventricular conduction abnormalities in a mouse myotonic dystrophy model. J Clin Invest 103:R1–R7.

Bleoo S, Sun X, Hendzel MJ, Rowe JM, Packer M, Godbout R. 2001. Association of human DEAD box protein DDX1 with a cleavage stimulation factor involved in 3′-end processing of pre-MRNA. Mol Biol Cell 12:3046–3059.

Brook JD, McCurrach ME, Harley HG, Buckler AJ, Church D, Aburatani H, Hunter K, Stanton VP, Thirion JP, Hudson T, et al. 1992. Molecular basis of myotonic dystrophy: expansion of a trinucleotide (CTG) repeat at the 3′ end of a transcript encoding a protein kinase family member. Cell 68:799–808.

Chernukhin IV, Shamsuddin S, Robinson AF, Carne AF, Paul A, El-Kady AI, Lobanenkov VV, Klenova EM. 2000. Physical and functional interaction between two pluripotent proteins, the Y-box DNA/RNA-binding factor, YB-1, and the multivalent zinc finger factor, CTCF. J Biol Chem 275:29915–29921.

Cordin O, Banroques J, Tanner NK, Linder P. 2006. The DEAD-box protein family of RNA helicases. Gene 367:17–37.

Davis BM, McCurrach ME, Taneja KL, Singer RH, Housman DE. 1997. Expansion of a CUG trinucleotide repeat in the 3′ untranslated region of myotonic dystrophy protein kinase transcripts results in nuclear retention of transcripts. Proc Natl Acad Sci U S A 94:7388–7393.

Day JW, Ricker K, Jacobsen JF, Rasmussen LJ, Dick KA, Kress W, Schneider C, Koch MC, Beilman GJ, Harrison AR, Dalton JC, Ranum LP. 2003. Myotonic dystrophy type 2: molecular, diagnostic and clinical spectrum. Neurology 60:657–664.

Fardaei M, Larkin K, Brook JD, Hamshere MG. 2001. In vivo colocalisation of MBNL protein with DMPK expanded-repeat transcripts. Nucleic Acids Res 29:2766–2771.

Fardaei M, Rogers MT, Thorpe HM, Larkin K, Hamshere MG, Harper PS, Brook JD. 2002. Three proteins, MBNL, MBLL and MBXL, colocalize in vivo with nuclear foci of expanded-repeat transcripts in DM1 and DM2 cells. Hum Mol Genet 11:805–814.

Fu YH, Friedman DL, Richards S, Pearlman JA, Gibbs RA, Pizzuti A, Ashizawa T, Perryman MB, Scarlato G, Fenwick RG Jr, et al. 1993. Decreased expression of myotonin-protein kinase messenger RNA and protein in adult form of myotonic dystrophy. Science 260:235–238.

Goodier JL, Zhang L, Vetter MR, Kazazian HH Jr. 2007. LINE-1 ORF1 protein localizes in stress granules with other RNA-binding proteins, including components of RNA interference RNA-induced silencing complex. Mol Cell Biol 27:6469–6483.

Gregory RI, Yan KP, Amuthan G, Chendrimada T, Doratotaj B, Cooch N, Shiekhattar R. 2004. The microprocessor complex mediates the genesis of microRNAs. Nature 432:235–240.

Harper PS. 2001. Myotonic dystrophy, 3rd ed., London: W.B. Saunders.

Ho TH, Charlet BN, Poulos MG, Singh G, Swanson MS, Cooper TA. 2004. Muscleblind proteins regulate alternative splicing. EMBO J 23:3103–3112.

Houseley JM, Wang Z, Brock GJ, Soloway J, Artero R, Perez-Alonso M, O'Dell KM, Monckton DG. 2005. Myotonic dystrophy associated expanded CUG repeat muscleblind positive ribonuclear foci are not toxic to *Drosophila*. Hum Mol Genet 14:873–883.

Jansen G, Groenen PJ, Bachner D, Jap PH, Coerwinkel M, Oerlemans F, van den Broek W, Gohlsch B, Pette D, Plomp JJ, Molenaar PC, Nederhoff MG, van Echteld CJ, Dekker M, Berns A, Hameister H, Wieringa B. 1996. Abnormal myotonic dystrophy protein kinase levels produce only mild myopathy in mice. Nat Genet 13:316–324.

Kanadia RN, Shin J, Yuan Y, Beattie SG, Wheeler TM, Thornton CA, Swanson MS. 2006. Reversal of RNA missplicing and myotonia after muscleblind overexpression in a mouse poly(CUG) model for myotonic dystrophy. Proc Natl Acad Sci U S A 103:11748–11753.

Kedersha N, Chen S, Gilks N, Li W, Miller IJ, Stahl J, Anderson P. 2002. Evidence that ternary complex (eIF2-GTP-tRNA(i)(Met))-deficient preinitiation complexes are core constituents of mammalian stress granules. Mol Biol Cell 13:195–210.

Kim SH, Dong WK, Weiler IJ, Greenough WT. 2006. Fragile X mental retardation protein shifts between polyribosomes and stress granules after neuronal injury by arsenite stress or in vivo hippocampal electrode insertion. J Neurosci 26:2413–2418.

Kino Y, Mori D, Oma Y, Takeshita Y, Sasagawa N, Ishiura S. 2004. Muscleblind protein, MBNL1/EXP, binds specifically to CHHG repeats. Hum Mol Genet 13:495–507.

Klenova E, Scott AC, Roberts J, Shamsuddin S, Lovejoy EA, Bergmann S, Bubb VJ, Royer HD, Quinn JP. 2004. YB-1 and CTCF differentially regulate the 5-HTT polymorphic intron 2 enhancer which predisposes to a variety of neurological disorders. J Neurosci 24:5966–5973.

Kohno K, Izumi H, Uchiumi T, Ashizuka M, Kuwano M. 2003. The pleiotropic functions of the Y-box-binding protein, YB-1. Bioessays 25:691–698.

Lin JC, Hsu M, Tarn WY. 2007. Cell stress modulates the function of splicing regulatory protein RBM4 in translation control. Proc Natl Acad Sci U S A 104:2235–2240.

Liquori CL, Ricker K, Moseley ML, Jacobsen JF, Kress W, Naylor SL, Day JW, Ranum LP. 2001. Myotonic dystrophy type 2 caused by a CCTG expansion in intron 1 of ZNF9. Science 293:864–867.

Mahadevan M, Tsilfidis C, Sabourin L, Shutler G, Amemiya C, Jansen G, Neville C, Narang M, Barcelo J, O'Hoy K, et al. 1992. Myotonic dystrophy mutation: an unstable CTG repeat in the 3′ untranslated region of the gene. Science 255:1253–1255.

Mankodi A, Logigian E, Callahan L, McClain C, White R, Henderson D, Krym M, Thornton CA. 2000. Myotonic dystrophy in transgenic mice expressing an expanded CUG repeat. Science 289:1769–1773.

Mankodi A, Urbinati CR, Yuan QP, Moxley RT, Sansone V, Krym M, Henderson D, Schalling M, Swanson MS, Thornton CA. 2001. Muscleblind localizes to nuclear foci of aberrant RNA in myotonic dystrophy types 1 and 2. Hum Mol Genet 10:2165–2170.

Meola G, Sansone V, Perani D, Scarone S, Cappa S, Dragoni C, Cattaneo E, Cotelli M, Gobbo C, Fazio F, Siciliano G, Mancuso M, Vitelli E, Zhang S, Krahe R, Moxley RT. 2003. Executive dysfunction and avoidant personality trait in myotonic dystrophy type 1 (DM-1) and in proximal myotonic myopathy (PROMM/DM-2). Neuromuscul Disord 13:813–821.

Miller JW, Urbinati CR, Teng-Umnuay P, Stenberg MG, Byrne BJ, Thornton CA, Swanson MS. 2000. Recruitment of human muscleblind proteins to (CUG)(n) expansions associated with myotonic dystrophy. EMBO J 19:4439–4448.

Miwa A, Higuchi T, Kobayashi S. 2006. Expression and polysome association of YB-1 in various tissues at different stages in the lifespan of mice. Biochim Biophys Acta 1760:1675–1681.

Nashchekin D, Zhao J, Visa N, Daneholt B. 2006. A novel Ded1-like RNA helicase interacts with the Y-box protein ctYB-1 in nuclear mRNP particles and in polysomes. J Biol Chem 281:14263–14272.

Pascual M, Vicente M, Monferrer L, Artero R. 2006. The Muscleblind family of proteins: an emerging class of regulators of developmentally programmed alternative splicing. Differentiation 74:65–80.

Raffetseder U, Frye B, Rauen T, Jurchott K, Royer HD, Jansen PL, Mertens PR. 2003. Splicing factor SRp30c interaction with Y-box protein-1 confers nuclear YB-1 shuttling and alternative splice site selection. J Biol Chem 278:18241–18248.

Rapp TB, Yang L, Conrad EU 3rd, Mandahl N, Chansky HA. 2002. RNA splicing mediated by YB-1 is inhibited by TLS/CHOP in human myxoid liposarcoma cells. J Orthop Res 20:723–729.

Reddy S, Smith DB, Rich MM, Leferovich JM, Reilly P, Davis BM, Tran K, Rayburn H, Bronson R, Cros D, Balice-Gordon RJ, Housman D. 1996. Mice lacking the myotonic dystrophy protein kinase develop a late onset progressive myopathy. Nat Genet 13:325–335.

Roberts J, Scott AC, Howard MR, Breen G, Bubb VJ, Klenova E, Quinn JP. 2007. Differential regulation of the serotonin transporter gene by lithium is mediated by transcription factors, CCCTC binding protein and Y-box binding protein 1, through the polymorphic intron 2 variable number tandem repeat. J Neurosci 27:2793–2801.

Stickeler E, Fraser SD, Honig A, Chen AL, Berget SM, Cooper TA. 2001. The RNA binding protein YB-1 binds A/C-rich exon enhancers and stimulates splicing of the CD44 alternative exon v4. EMBO J 20:3821–3830.

Taneja KL, McCurrach M, Schalling M, Housman D, Singer RH. 1995. Foci of trinucleotide repeat transcripts in nuclei of myotonic dystrophy cells and tissues. J Cell Biol 128:995–1002.

Vicente M, Monferrer L, Poulos MG, Houseley J, Monckton DG, O'Dell K M, Swanson MS, Artero RD. 2007. Muscleblind isoforms are functionally distinct and regulate alpha-actinin splicing. Differentiation 75:427–440.

Yang WH, Bloch DB. 2007. Probing the mRNA processing body using protein macroarrays and "autoantigenomics." RNA 13:704–712.

Young JI, Hong EP, Castle JC, Crespo-Barreto J, Bowman AB, Rose MF, Kang D, Richman R, Johnson JM, Berget S, Zoghbi HY. 2005. Regulation of RNA splicing by the methylation-dependent transcriptional repressor methyl-CpG binding protein 2. Proc Natl Acad Sci U S A 102:17551–17558.